GEOLOGY FOR SOCIETY

SINCE 1858

GEOLOGICAL
SURVEY OF
NORWAY

· NGU ·

NORGES GEOLOGISKE UNDERSØKELSE
· NGU ·

REPORT

Geological Survey of Norway
P.O.Box 6315 Torgarden
NO-7491 TRONDHEIM
Tel.: 47 73 90 40 00

Report no.: 2019.039	ISSN: 0800-3416 (print) ISSN: 2387-3515 (online)	Grading: Open

Title:
Reprocessing of airborne gamma-ray spectrometry data in Norway for mapping of Cs-137 deposition from the Chernobyl accident.

Authors: V.C. Baranwal, A. Stampolidis, J. Koziel, R.J. Watson and J.S. Rønning	Client: NGU - DSA
County: Innlandet, Trøndelag and Nordland	Commune:

Map-sheet name (M=1:250.000)	Map-sheet no. and -name (M=1:50.000)

Deposit name and grid-reference:	Number of pages: 61 Map enclosures:	Price (NOK): 200,-

Fieldwork carried out: 1987 - 2015	Date of report: 20.05.2020	Project no.: 366900	Person responsible: *Marco Brönner*

Summary:

A catastrophic nuclear accident occurred on April 26[th]1986 at Chernobyl nuclear power plant outside Kiev, Ukraine. Because of the accident, several areas in Norway received radioactive fallout. Initially, several anthropogenic radionuclides were present in the fallout. However, most of them disintegrated into stable isotopes due to their short half-life. Today, Cs-137 with a half-life of 11,000 days ($\approx$ 30 years) remains in significant quantities and may constitute a potential health hazard. If soil of these regions is not altered due to agriculture or other purposes, then Cs deposition remains intact and it is absorbed by flora and fauna.

Airborne data were collected by different surveys using helicopter and fixed-wing aircrafts during 1987 to 2015. Recalibration and reprocessing methods are demonstrated to correct low energy isotopes from U and Th decay chain appearing in Cs-137 window and to find a better correlation between airborne and *in situ* measurements. Recalibration data from Beitostølen, Jotunheimen brought estimation of Cs-137 from airborne measurements to almost equal to *in situ* measurements regardless of local variations and different scale of these two measurements. Therefore, all the airborne radiometry data from Nordland, Jotunheimen and Trøndelag, which got mostly affected after the Chernobyl nuclear accident, are reprocessed according to the new calibration and reprocessing procedures. Hattfjelldal and Jotunheimen data show that there are many areas that are still contaminated with high amount of Cs-137 (close to 100 kBq/m^2) even 30 years after the nuclear accident. Other areas of Nordland seems less contaminated. Trøndelag shows contamination of 20 to 50 kBq/m^2 in some areas while others are not contaminated.

Cs-137 deposition is calculated for actual survey year (1987-2015) and then concentration is decay-corrected for the year 2016 using half-life decay equation. There could be additional washing of the deposited Cs-137 or other changes due to agriculture or other activities in some of the areas. Therefore, the estimated 2016 Cs-137 concentration could be higher than the actual concentration of Cs-137 in such areas.

Keywords:	Geophysics	Radiometric method	Chernobyl accident
	Cs fallout	Calibration	Processing
		Cs ground concentration	Scientific report

CONTENTS

FIGURES

TABLES

1. INTRODUCTION

A catastrophic nuclear accident occurred on 26th April 1986 at Chernobyl nuclear power plant outside Kiev, Ukraine. As a consequence of the accident, several areas in Norway received radioactive fallout. Immediately after the accident in 1986, the Geological Survey of Norway (NGU) performed airborne and car-borne gamma-ray measurements in central Norway (Lindahl & Håbrekke 1986). At that time, it was not possible to calculate reliable radionuclide concentration, therefore data were presented as total counts per second. Results of the immediate measurements are presented in the next chapter.

Initially, several anthropogenic radionuclides were present in the fallout from the nuclear accident. However, most of them have disintegrated into stable isotopes due to their short half-life. Today, only caesium (i.e. Cs-137) with a half-life of 11,000 days (≈ 30 years) remains in significant quantities and may constitute a potential health hazard. If soil of these regions is not altered due to agriculture or other purposes, then Cs deposition remains intact and it is absorbed by flora and fauna.

Recently, NGU has collected new airborne gamma-ray spectrometry (AGRS) data over large areas using helicopter-borne and fixed-wing surveys to map bedrock geology and mineral potential through various state and county sponsored projects (e.g. *Mineral Resources in North Norway (MINN)* and *Mineral Resources in South Norway (MINS)*). The AGRS data are generally processed to prepare maps of the naturally occurring radioactive elements such as potassium, thorium and uranium. However, this data can also be used to calculate concentration of anthropogenic radioactive sources (e.g. Cs-137). Therefore, NGU proposed to the former *Statens Strålevern* (now *Norwegian Radiation and Nuclear Safety Authority*, DSA) to prepare, where possible, Cs-137 deposition maps from different parts of Norway using airborne gamma-ray spectrometry data.

In 2011, the Reindeer Husbandry Administration (now part of the County Governor) financed a joint effort with DSA and NGU to collect AGRS data by helicopter from the Jotunheimen area and to calculate the Cs-137 deposition (Baranwal et al. 2011). Follow-up work on the Jotunheimen Cs deposition map presented by Thørring & Skuterud (2012) indicated that the Cs deposition estimates obtained from the airborne survey had underestimated the Cs-137 deposition by a factor close to two (Thørring & Skuterud 2012). Thereafter, NGU proposed a project to recalibrate the instruments and to reprocess the Cs data to obtain high quality Cs deposition compilation. Until now, new Cs-137 maps are produced from the areas Jotunheimen-Otta-Vågå, Trøndelag and selected areas in Nordland County. This report documents the final processing procedure and the Cs deposition data quality.

Recalibration measurements of the AGRS data were done at Beitostølen in 2015 by NGU (Robin Watson and Alexandros Stampolidis) and DSA (Alexander Mauring and Marie Solberg). Vikas Baranwal and Alexandros Stampolidis reprocessed AGRS data for Cs-137 deposition. Janusz Koziel (NGU) recovered older AGRS data and converted them from binary coded spectrometer data to ascii format. Vikas Baranwal has stitched Cs grids from different old and new surveys and produced all the Cs maps and Jan S. Rønning has administrated the project from data acquisition to processing, calibration, map production and edited the report.

2. EARLIER PROCESSING AND PRESENTATION OF Cs DATA

In this chapter we present previous processing and presentation of Cs-137 data from the AGRS.

2.1 Immediate total count presentation after the Chernobyl accident

During the summer of 1986, just after the Chernobyl accident, NGU obtained funding to perform AGRS measurements in polluted areas of mid Norway (Lindahl & Håbrekke 1986). The first data were collected north of Trondheim using an army helicopter as an instrument carrier. In Southern Norway, the measurements were performed from a fixed-wing aircraft. Car-borne radiometric measurements were also performed at the same time. NGU was unable to perform the processing that could separate man-made deposition from the natural radiation source (K, U, Th) at that time. Therefore, AGRS data were presented as total counts including man-made and natural radiation. Due to the high deposition rate just after the Chernobyl accident, the maps presented in Figures 1 and 2 mostly represent man-made deposition.

In Figure 1 (Southern Norway) and Figure 2 (North of Trondheim), an interpolated grid map of total counts is overlain by total counts is shown along the measured lines. In this way, actual measured level (in counts per second) and measuring path is also indicated. The line spacing was sparse and flying altitude was high and very variable, especially in Southern Norway due to bad weather (Lindahl & Håbrekke 1986). It is obvious that this is not a high-quality presentation of the Chernobyl accident deposition, but it was an attempt to locate where deposition had occurred at that time.
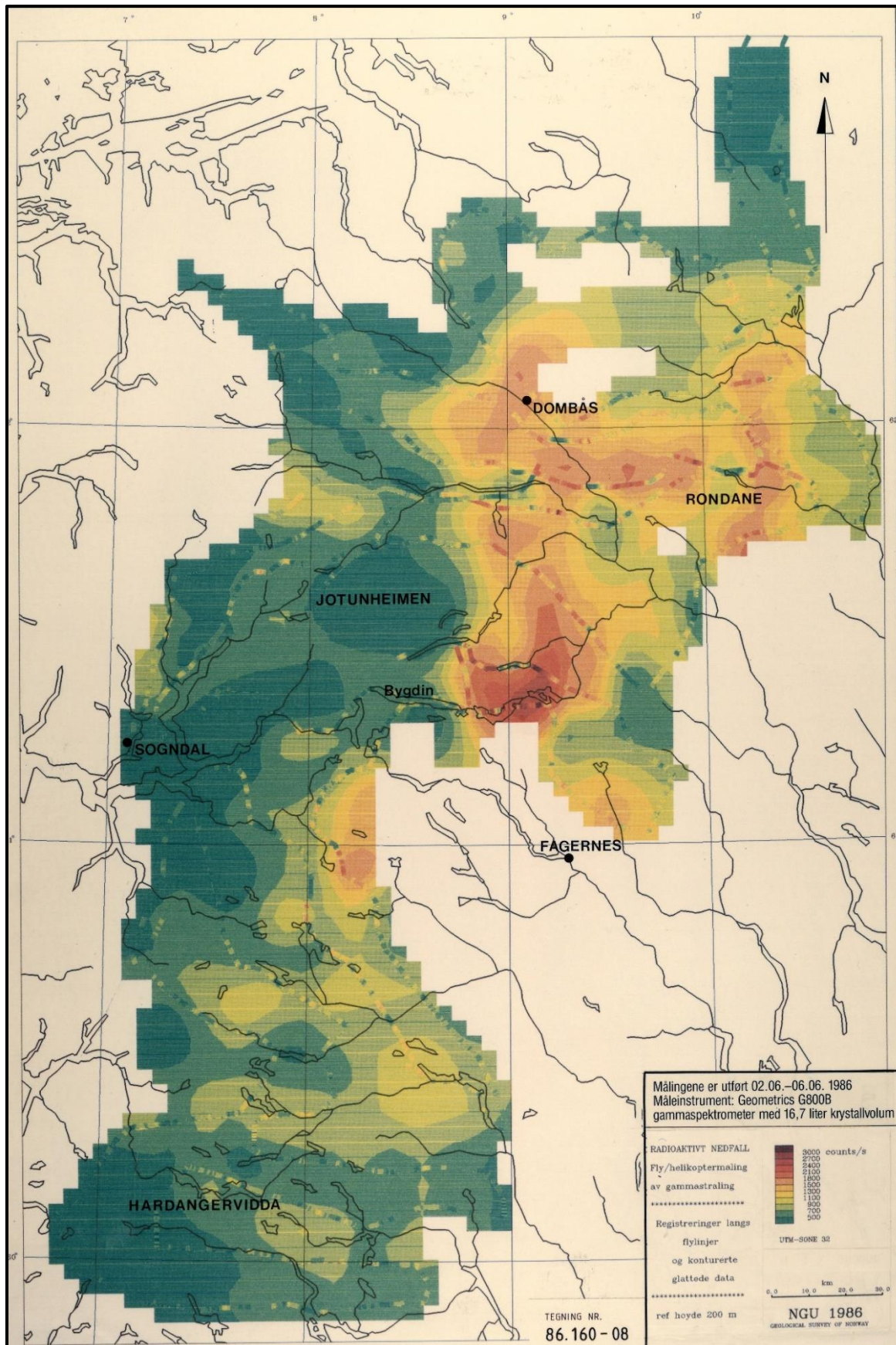
Figure 1: Deposition from the Chernobyl accident in total counts per second in Southern Norway from AGRS measurements using a fixed-wing aircraft in the summer of 1986. The coloured lines represent the measured data along the flight lines while the gridded data shows interpolated values from the measured data (From Lindahl & Håbrekke 1986).
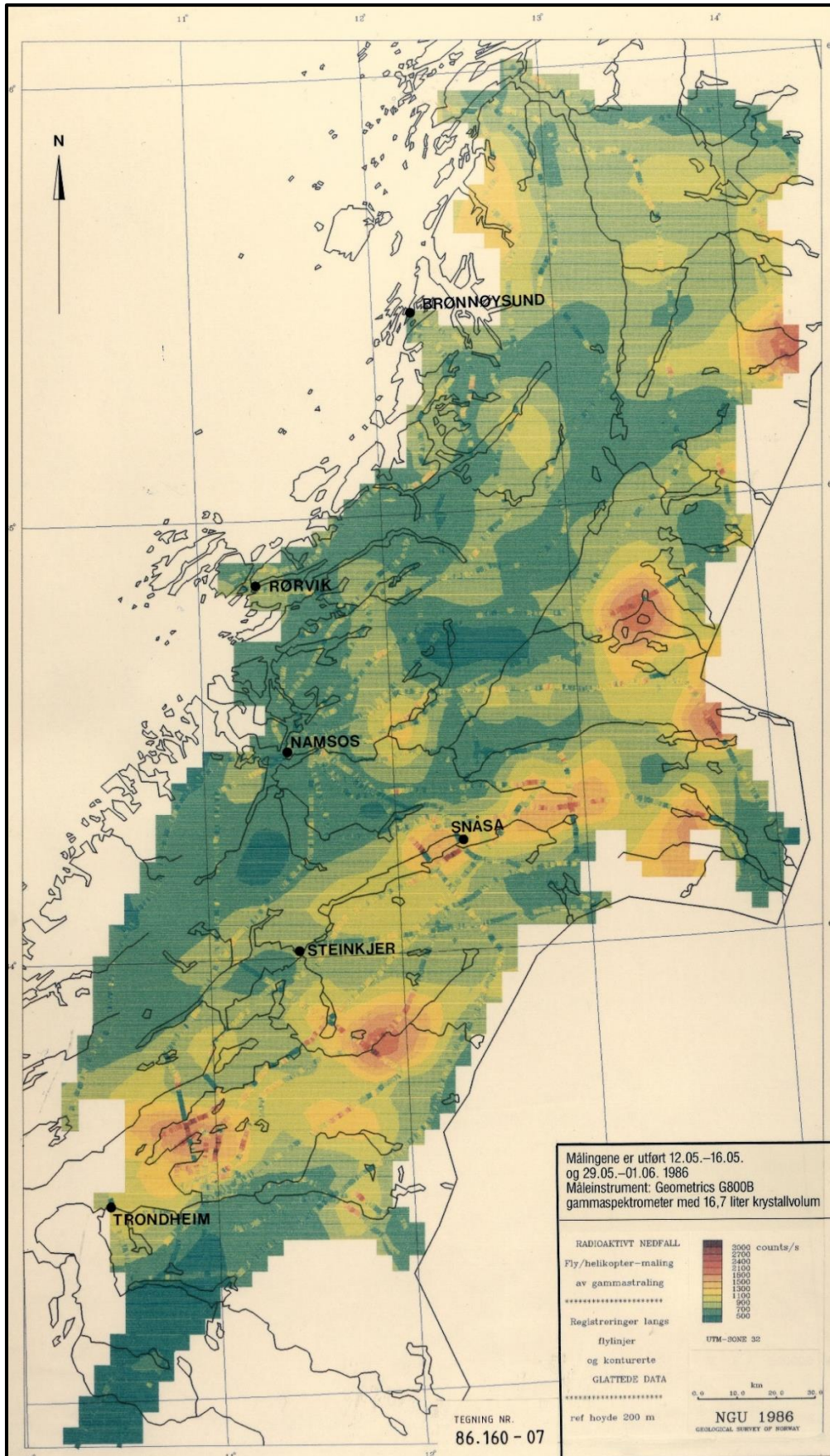
Figure 2: Deposition from the Chernobyl accident in counts per second north of Trondheim from AGRS measurements using a helicopter in the summer of 1986. The coloured lines represent the measured data along the flight lines while the gridded data shows interpolated values from the measured data (From Lindahl & Håbrekke 1986).

2.2 Earlier processing (2011) to calculate Cs-137 deposition

In this chapter, we present examples of window-based processing for Cs-137 where data apparently looks good but when critically examined showed methodological weaknesses.

2.2.1 Description of window-based processing

The spectrometry data collected in 2011 were processed following general guidelines of IAEA (IAEA 1991, 2003) for live time, aircraft background, cosmic correction, radon and stripping correction. Sensitivity coefficient calculation was done using a point source (for Cs-137) and calibration pads (for K, U and Th) instead of a test site as suggested in IAEA (1991, 2003). Details of the processing are described in Baranwal et al. (2011). Calibration data collected on calibration pads at ground level at NGU were used to calculate the standard stripping ratios for each of K, U and Th into the Cs window. A ground-level sensitivity factor for Cs-137 was estimated using a Cs-137 source (activity 433 kBq). The Cs-137 source was moved over a 1 m grid pattern on the ground, with the detector positioned 0.9 m above the ground. The counts in the Cs-137 window at the detector for each measurement point were summed to approximate the response to an infinite ground source with surface concentration 433 kBq/m^2 (Walker & Smethurst 1993). The resultant sensitivity S_0 can be expressed as (equation 1):

$$\text{Sensitivity } (S_0) = \frac{Cs \text{ window counts } (Cs^{counts})}{Cs \text{ Concentration } (Cs^{conc})}, \quad \text{..(1)}$$

where Cs^{counts} is the background-corrected counts in the Cs-137 window (here defined as 612 keV to 712 keV) summed over all the grid measurement points, and Cs^{conc} is the activity of the Cs-137 point source. Previously, Baranwal et al. (2011) calculated a height attenuation coefficient μ for Cs-137 following IAEA (2003) from calibration flights between 40 m to 80 m and obtained an exponential height attenuation factor of 0.0088 per meter. Equation (2) was used to convert ground sensitivity to nominal flying altitude sensitivity, assuming the same exponential attenuation would be valid from the ground to the flying altitude.

$$S_h = S_{h_0} e^{-\mu(h-h_0)}, \quad \text{...(2)}$$

where S_h is the desired sensitivity at nominal height h and S_{h_0} is the sensitivity calculated at initial height h_0 or at ground ($h_0 = 0$).

The calculated sensitivity coefficients at the flying altitude and the processed Cs window counts at flying altitude were used to calculate the ground concentration of Cs-137 using equation (1).

Figure 3 shows a typical gamma-ray spectrum without and with Cs-137 and natural radioactive sources. The Cs window contains a direct contribution from 208Tl and 214Bi photo-peaks (from thorium and uranium decay chains respectively) in addition to Compton scattering from potassium, uranium and thorium decay products. Insufficient stripping of natural radioactive elements (i.e. U and Th) from Cs window

has caused a challenge in calculation of accurate Cs-137 ground concentration, especially for low Cs-137 concentration areas where the distribution pattern of natural radioactive elements (U and Th) is visible in the calculated Cs-137 deposition.
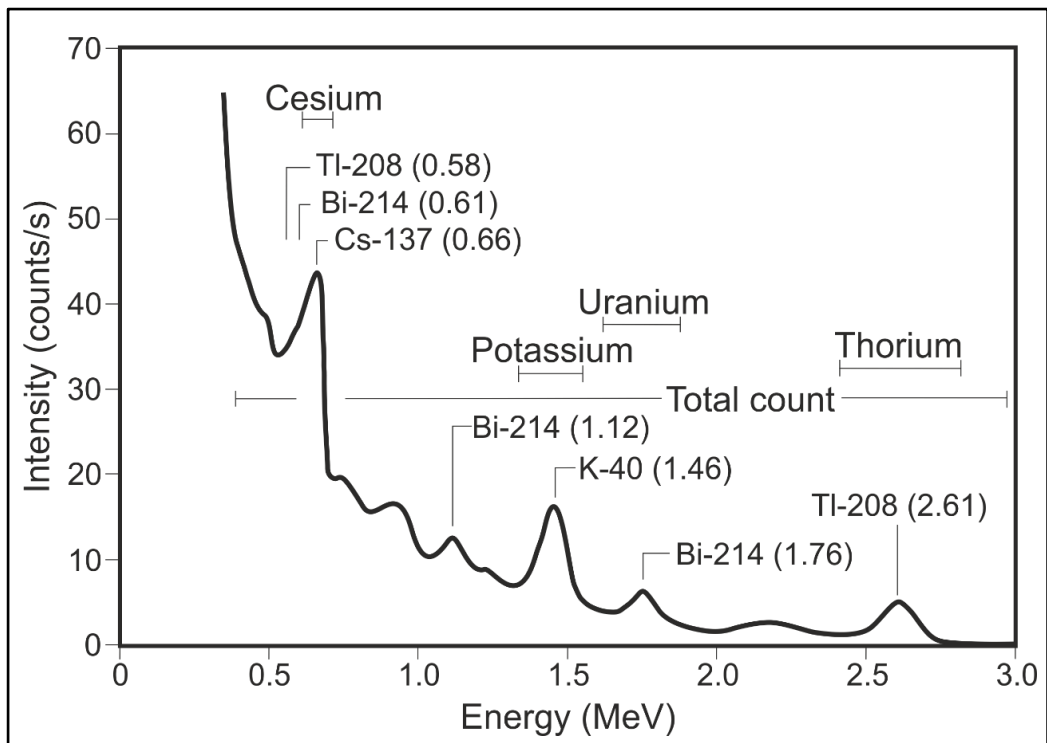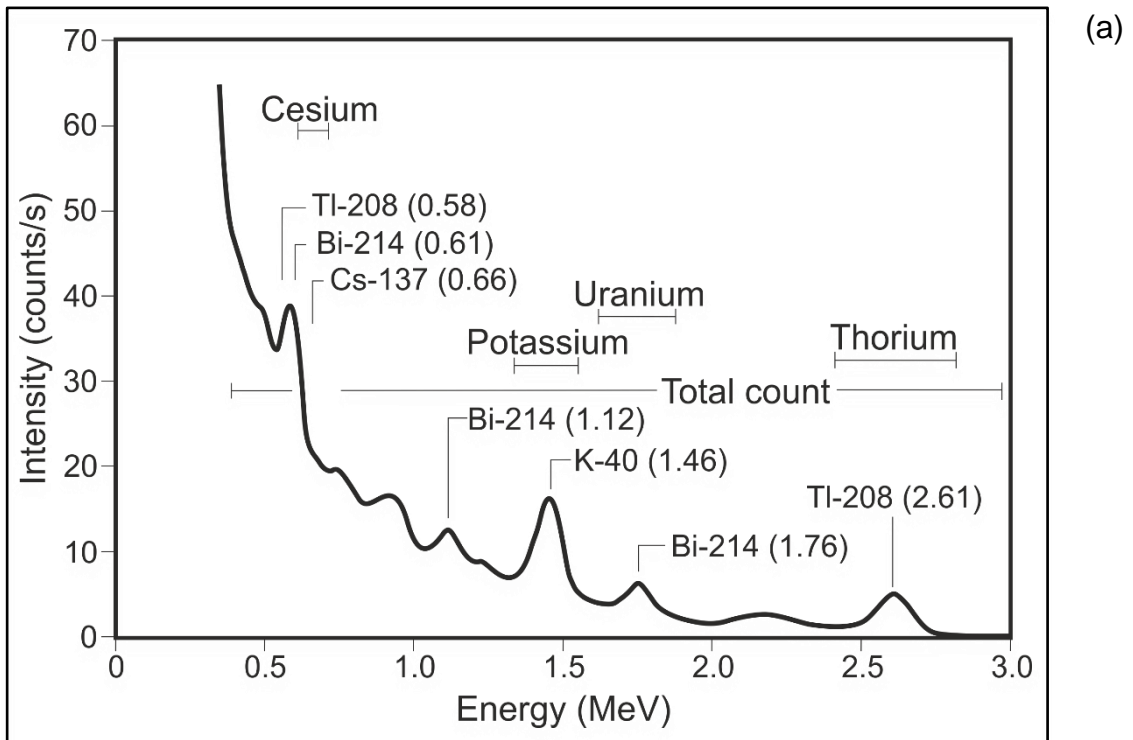
Figure 3: A typical gamma-ray spectrum showing windows and energy peaks for Th, U, K and its isotopes (a) without any Cs-137 peak and (b) with a Cs-137 peak (Modified after Wilford, 2002).

2.2.2 Cs deposition from the Jotunheimen area

In 2011, NGU collected gamma-ray spectrometry data by helicopter from the Jotunheimen area to map the Cs deposition in some of the most contaminated reindeer grazing areas for the Reindeer Husbandry Administration (now County Governor). A Cs deposition map of the Jotunheimen area obtained from windows-based processing, and decay-corrected to 1st June 2011 is shown in Figure 4 (after Baranwal et al. 2011).
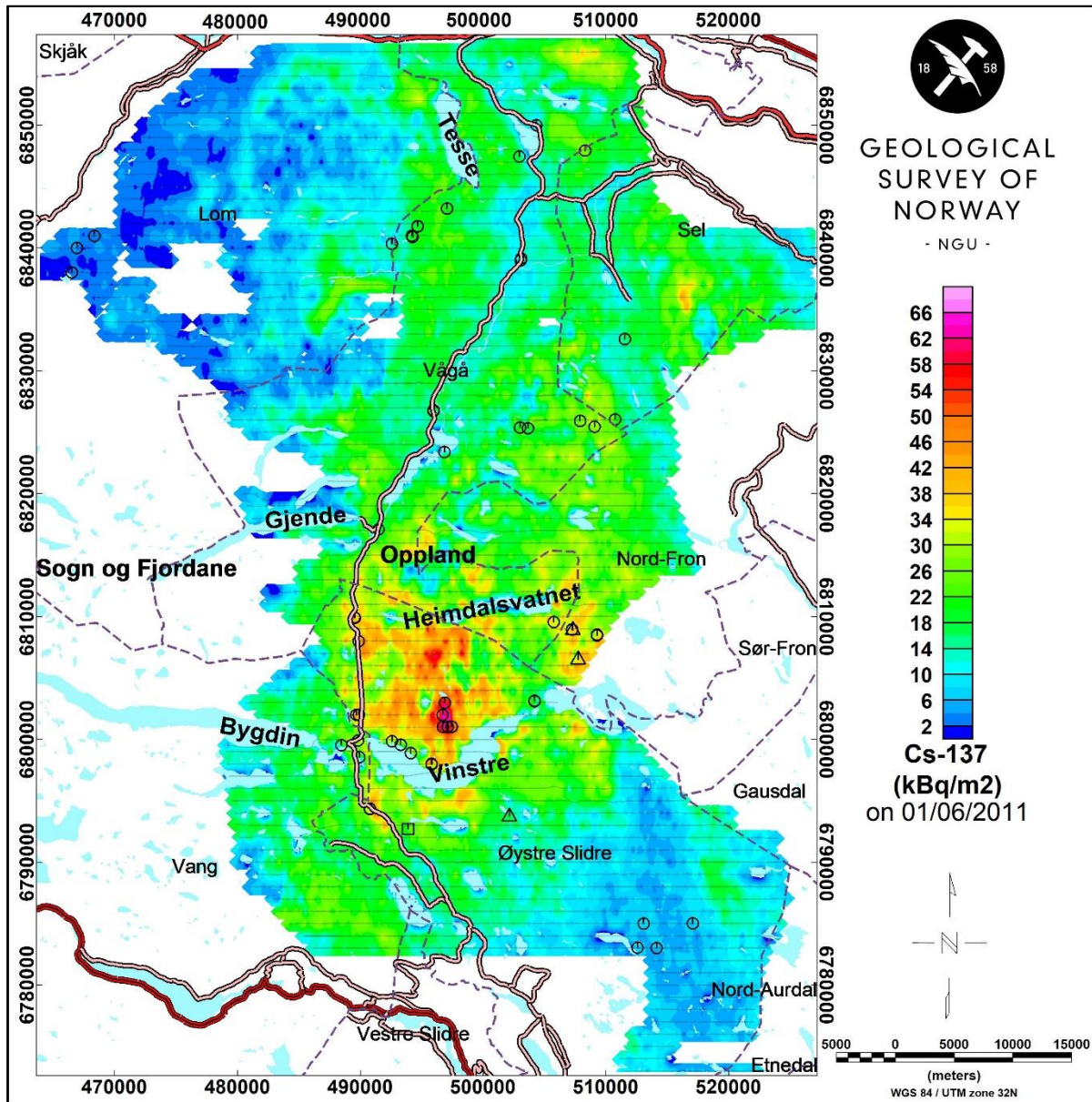
Figure 4: Caesium map of the Jotunheimen area decay corrected to 1st June 2011 with linear distribution plotting (after Baranwal et al. 2011). Blank area in the north west is showing absence of the data over parts of Jotunheimen highland park. Water bodies are also overlaid in the image in semi-transparent light blue colour. The circles show in situ measurements and soil sample locations between 2001 to 2016 by DSA. The triangles mark the location of calibration sites in 2011 for hand-held spectrometer used in in-situ measurements in 2012 and 2016. The rectangle marks the site used for the 2015 helicopter recalibration survey.

15

2.3 Comparing aerial and ground-based measurements from Jotunheimen

The following year, in 2012, DSA conducted several *in-situ* measurements using the instrument *Inspector 1000* positioned 1 m above the ground, together with laboratory analyses of soil to determine Cs deposition across the airborne survey area (Thørring et al. 2019). The calibration sites for the *Inspector 1000 in-situ* measurements in 2012 are shown by the triangles in Figure 4. Details of the calibration for *Inspector 1000* spectrometer and soil sample analyses are described by Mauring et al. (2017) and Thørring et al. (2019), respectively. Location of *in-situ* measurements and soil samples (together with older measurements before 2010 and newer measurements in 2016) are shown by circles in Figure 4. A preliminary comparison of *in situ* gamma spectrometry measurements and soil samples (analysed in the laboratory) from 2011 and 2012 (20 measurements) indicated that the Cs-137 deposition estimates obtained from the airborne survey had underestimated the Cs-137 deposition (see Figure 5). The deposition from ground measurements and soil analysis were around 1.6 times higher than the deposition estimated from helicopter-borne measurements. We suspected that underestimated Cs-137 deposition calculated from airborne survey in Jotunheimen could be mainly due to two factors: 1) incorrect stripping and 2) incorrect instrument sensitivity coefficient.
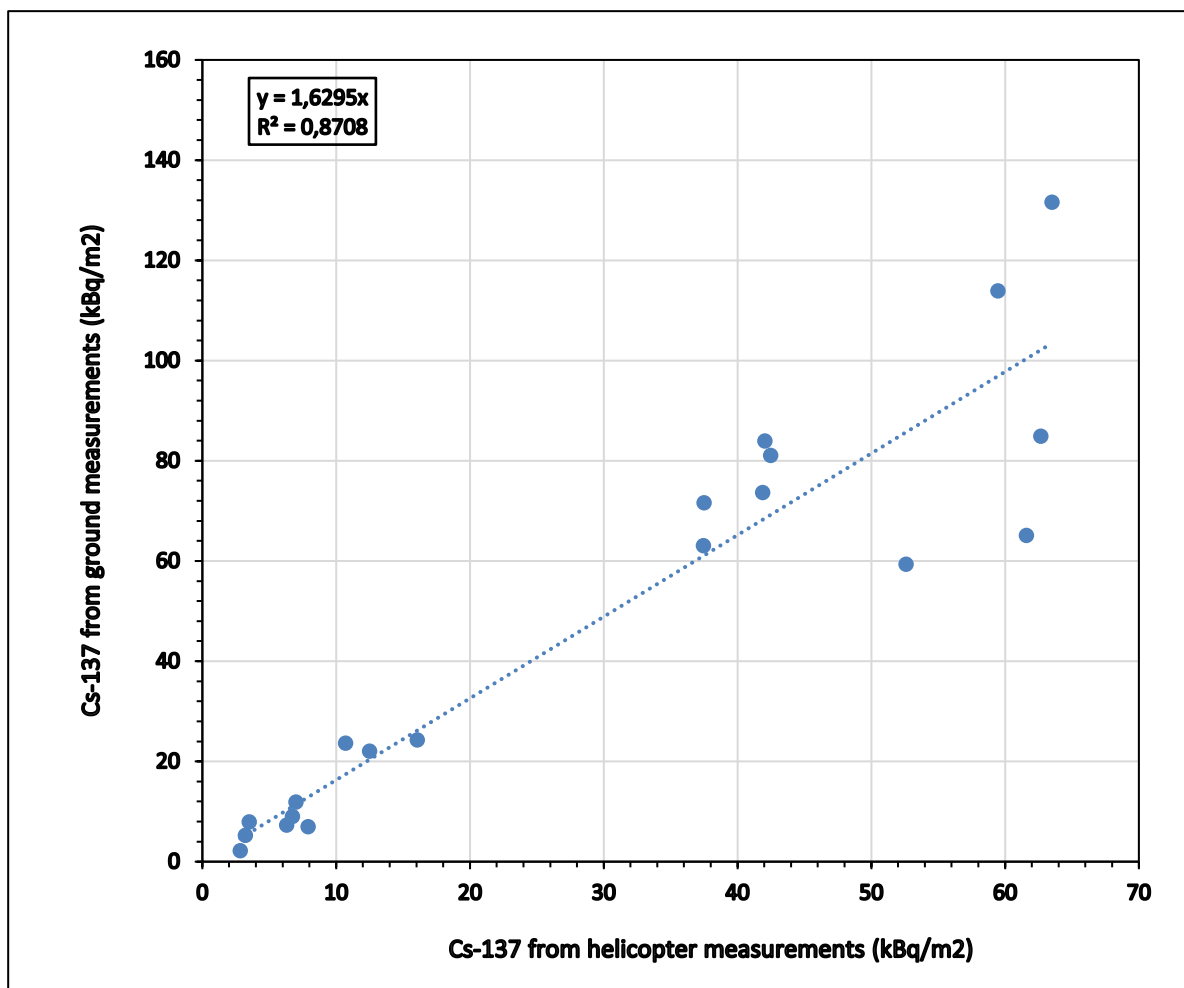
Figure 5: Cs concentrations from the helicopter-borne survey vs. ground measurements and soil analyses (2011-2012) in Jotunheimen.

2.4 Cs deposition from Hattfjelldal and Drangedal: effect of incorrect stripping

During the years 2011 to 2015 NGU performed several helicopter-borne surveys in Northern and Southern Norway under the projects MINN and MINS. Cs-137 concentrations using the traditional processing (described in Chapter 2.2.1) were performed in two areas: Hattfjelldal in the MINN area and Drangedal in the MINS area. Data acquisition and processing in these areas are described in NGU reports (Rodionov et al. 2014 and Stampolidis & Ofstad 2015). Cs-137 concentrations were compared with the concentrations of equivalent uranium (eU). Concentration of uranium (U) and thorium (Th) are defined as equivalent uranium (eU) and equivalent thorium (eTh) because they are not calculated directly from uranium and thorium itself but from measurements of their decay products (e.g. Bi-214 for U and Tl-208 for Th) assuming radioactive equilibrium in the decay series. Figures 6 and 7 show Cs-137 and eU concentrations from standard processing from Hattfjelldal area in North Norway and Drangedal area in South Norway, respectively.
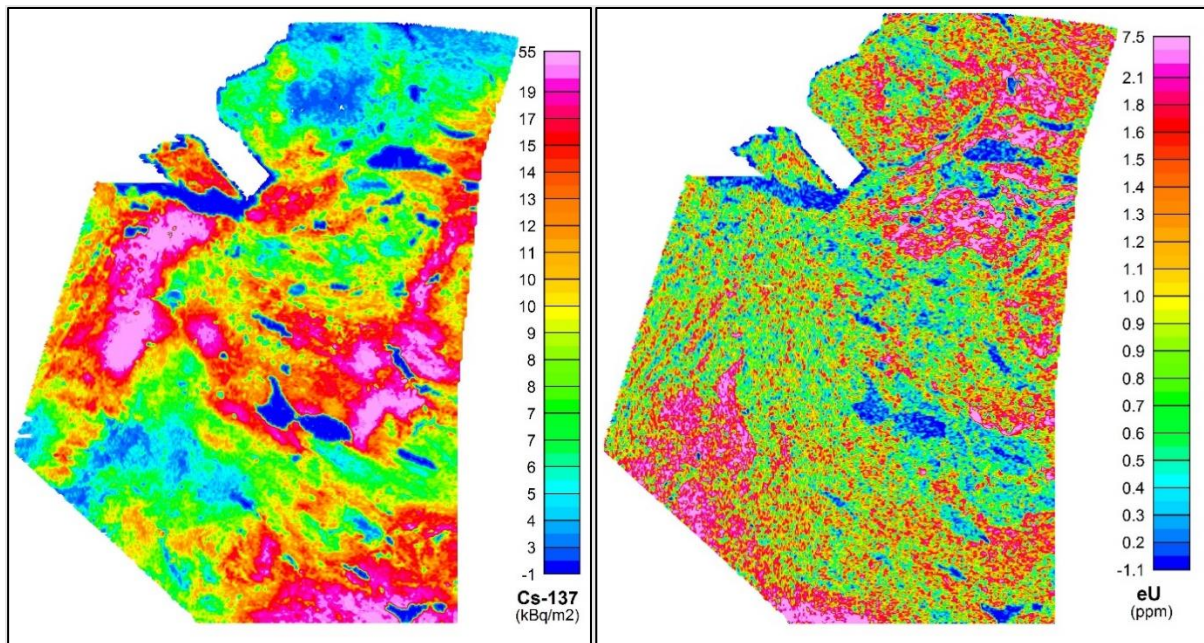
Figure 6: Ground Cs-137 concentration (left) and ground eU concentration (right) after standard processing of data from Hattfjelldal (Northern Norway).
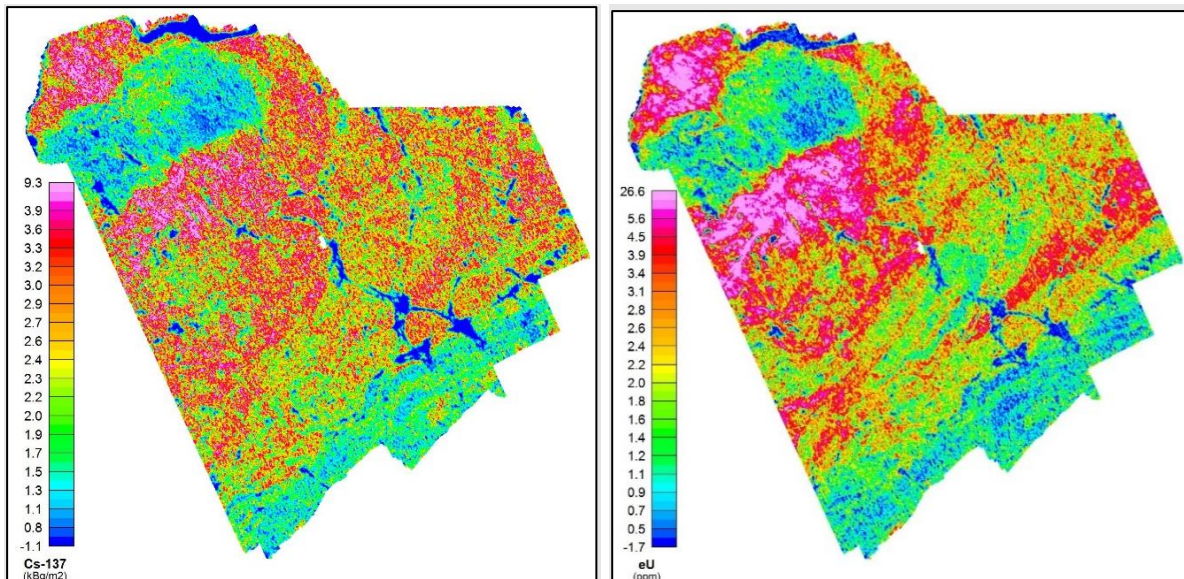
Figure 7: Ground Cs-137 concentration (left) and ground eU concentration (right) after standard processing of data from Drangedal (Southern Norway).

In Hattfjelldal, the maximum Cs-137 concentration was calculated to 55 kBq/m² and the maximum eU concentration 7.5 ppm. In this area we see a distinct difference in the Cs and eU anomaly pattern. If the Cs concentration is high enough (e.g. > 20 kBq/m²) compared to the eU concentration (e.g. < 5 ppm) as in Hattfjelldal, then no influence of natural U (or Th) is visible in the Cs ground concentration. On the other hand, if Cs-137 concentration is low (e.g. < 5 kBq/m²) and the eU concentration high (e.g. > 5 ppm) then Cs and eU show similar patterns as shown in Figure 7 from Drangedal. This indicates that the effect of natural occurring radioactive elements are not fully removed from the Cs window. It is mainly because the gamma radiations from Tl-208 in the Th decay chain and gamma radiations from Bi-214 in the U decay chain, together with Compton continuum are not fully removed from the Cs window (see Figure 3). Therefore, a new processing procedure described in the next chapter is considered to improve the data quality.

2.5 Contribution of soil depth distribution in Cs-137 activity: effect of incorrect sensitivity coefficient

Earlier sensitivity coefficient for Cs-137 was calculated using a point source placed in a gridded pattern. This way the Cs-137 concentration was calculated only from the surface and any contribution generated due to Cs-137 in the soil from various depths were ignored. Mauring (2016) and Thørring et al. (2019) showed that 91-97 % of the Cs-137 activity was contributed from 0-3 cm soil layer in the Jotunheimen area. Mauring (2016) argued that density of the soil in Jotunheimen was ca. 1.5 g/cm³ and relaxation length of the soil was ca. 2 cm at Beitostølen which gave a relaxation mass depth of 3 g/cm². Generally, soil depth distribution follows an exponential decay with depth (ICRU 1994). Relative photon flux (or activity) at different detector heights for a pure surface distribution and a real exponential depth distribution are provided by ICRU (1994). This relaxation mass depth value (i.e. 3 at Beitostølen) will lead to a geometrical factor ca. 2 for a plane surface model (no contribution from the depth) in comparison to a real exponential depth distribution for a detector placed at 1 m height from the surface (pers. comm. with Alexander Mauring (2019), formerly at DSA and

18

now at IAEA). This is likely to be one of the main reasons why the point source method underestimated the Cs-137 concentration with almost a factor of 2.

2.6 A brief summary on previous processing

Calibration test in the Jotunheimen area showed that the ground Cs-137 concentration measured from a helicopter was much less than the Cs-137 concentrations on the ground measured by well calibrated hand-held spectrometers and from analysed soil samples in the laboratory. In Hattfjelldal, the distribution pattern of Cs-137 ground concentration measured from helicopter was apparently correct. However, in Drangedal with low Cs concentration, the Cs-137 concentration shows a strong influence of naturally occurring U (and Th). These observations led NGU to carry out a recalibration and reprocessing of the helicopter-borne gamma ray spectrometer data for the Cs-137 concentration to achieve a better correlation of measured ground concentrations of Cs-137 by helicopter-borne and ground-based spectrometers.

3. RECALIBRATION AND NEW PROCESSING PROCEDURE

In this chapter a recalibration and new processing procedure adapted in 2015 for calculation of Cs-137 deposition from the airborne gamma ray spectrometry (AGRS) data is described.

3.1 Recalibration of helicopter-borne survey with ground measurements for Cs-137

Airborne survey calibrations are typically carried out by establishing a test-line or test-site which is flown over by airplane or helicopter (IAEA 2003). The site is surveyed with hand-held spectrometers to establish ground concentrations. Sensitivity coefficient to calculate concentration of radionuclides of interest are determined by taking the ratio of observed counts-per-second at desired survey height to the ground concentrations (IAEA 1991, 2003). Grasty and Minty (1995) and IAEA (1991, 2003) outline procedures and recommendations for calibration sites, and Tyler et al. (1996) describe in detail a procedure for calibration of helicopter-borne surveys at a test site. We adopted an approach similar to Tyler et al. (1996) here, an approach which takes better account of possible inhomogeneities in the calibration area. For the new recalibration in 2015, we selected a location next to Beitostølen in the southern part of Jotunheimen area (shown by a rectangle in Figure 4).

The calibration site at Beitostølen met the following requirements:
1. Relatively high and uniform concentrations of Cs-137 and the main natural radioelements (U, Th and K)
2. Relatively flat terrain extending at least 200 m radius around the centre of calibration
3. Proximity to a large water body for background and radon correction measurements

The site was surveyed with a hand-held gamma-ray spectrometer (Mauring 2017) using a hexagonal sampling pattern as shown in Figure 8. Hand-held measurements were performed over a period of several hours together with helicopter-borne measurements on the same day.

3.1.1 Ground measurements using hand-held spectrometers

A hexagonal sampling pattern was set up as indicated in Figure 8 with sampling points at 8, 32, 64, and 128 m distance from the centre of the sampling site. In-situ spectrometry measurements were performed by DSA at each sampling site using handheld spectrometers *Inspector 1000* NaI instruments (Canberra), placed 1 m above the ground, and with a measurement time of 600 seconds. The Inspector instruments were calibrated for Cs ground concentrations using InSiCal (Mauring et al. 2017). Background data were collected over a nearby lake (Øyangen) by taking the detectors out in fibre-glass canoes, at least 100 m away from the shoreline, and collecting the data for 900 seconds.
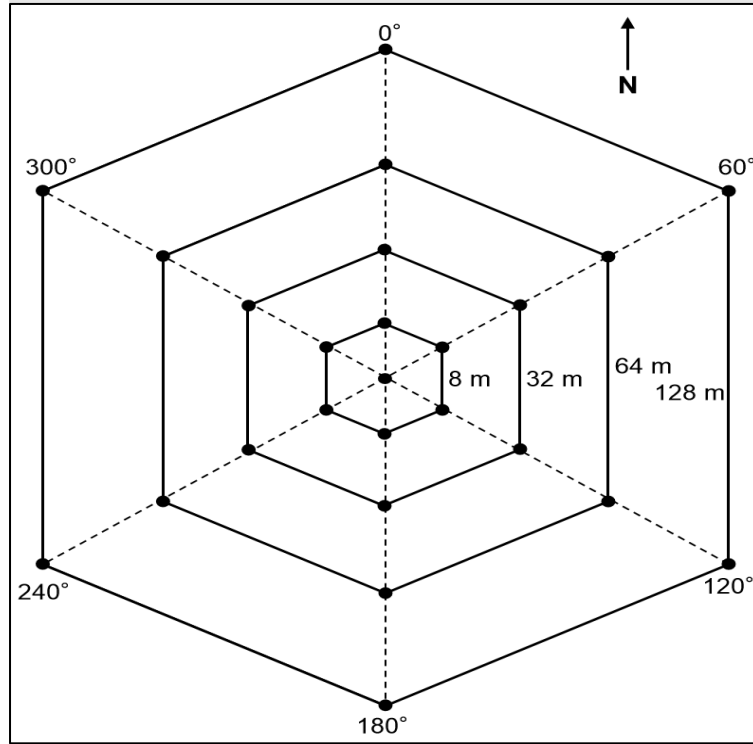
Figure 8: Schematic image of measured points around the calibration site using a calibrated hand-held gamma spectrometer.

To account for different contributions of sample points to the field of view of the airborne detectors, each point was given a weighting factor, using a method based on Tyler et al. (1996). The midpoints between the 8 m, 32 m, 64 m and 128 m sample distances were used to define circles of radius 20 m, 48 m and 96 m. The 8 m sample points were assumed representative of the inner 20 m radius circle and were given a weighting factor based on the fraction of infinite plane radiation originating from this circle. Similarly, the sample points at 32 m and 64 m distance were assumed to be representative of the rings formed between the 20 m and 48 m circles, and between the 48 m and 96 m circles, respectively, and were given weighting factors based on the fraction of infinite plane radiation originating from these rings. The remaining sample points (at 128 m) were given the residual weighting such that all weighting factors sum to 1. Sample points at 128 m distance were assumed to represent the contribution from 96 m onwards to infinity. The contribution of each ring was calculated by multiplying the measured activity density by the weighting.

The fraction of infinite plane radiation originating from a ring of a given radius is calculated using relationships described in Isaksson (2011) for photon fluence rates and disc geometries and is outlined here.

The photon fluence rate Φ at a height h above an infinite plane is given by equation 3 (equation 35 from Isaksson (2011)):

$$\Phi = \frac{S}{2}[E(\mu h)] \tag{3},$$

where E is the exponential integral function $(E(\mu h) = \int_{\mu h}^{\infty} \frac{e^{-t}}{t} dt)$, and $t = \mu h / \cos \alpha$. S for our purposes can be considered proportional to the surface concentration of photon emitters, and μ is the air attenuation factor for photons of the energy of interest.

The photon fluence rate at a height h above a disc subtending a half-angle α at the detector (Figure 9) will be given by equation 4 (i.e. equation 34 from Isaksson (2011))

$$\Phi = \frac{S}{2}\left[E(\mu h) - E\left(\frac{\mu h}{\cos\alpha}\right)\right] \tag{4},$$
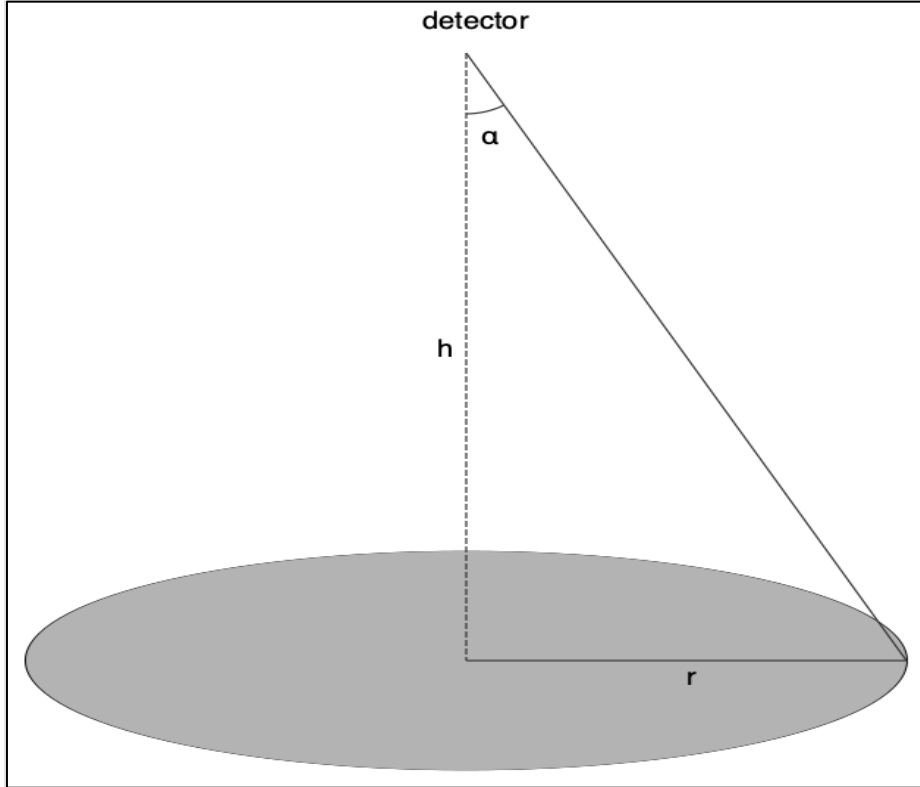
Figure 9: Footprint of a radiometric measurement at a height h over the surface. (adapted from Isaksson, 2011).

The fraction of infinite plane radiation originating from a disc will therefore be the ratio of terms on the right-hand sides of equations 3 and 4, and will be:

$$f = \frac{E(\mu h) - E\left(\frac{\mu h}{\cos\alpha}\right)}{E(\mu h)} \tag{5}.$$

Using equation 5, and assuming an air attenuation factor $\mu = 0.01005$ per meter and a survey height $h = 60$ m, we obtain weighting factors per ring and per sample point given in Table 1. The fractional contributions per point are obtained by dividing the contribution for each ring by six.

Table 1: Fractional contribution of each measuring point shown in Figure 8.

Sample point distance (m)	Inner radius (m)	Outer radius (m)	Ring contribution (%)	Fractional contribution per point
8	0	20	10.1	0.017
32	20	48	30.3	0.051
64	48	96	36.2	0.060
128	96	infinity	23.4	0.039

Cs surface concentrations from in-situ measurements and weighted Cs concentrations (Cs concentration multiplied by fractional contribution) are shown in Table 2. The weighted sum 37.16 kBq/m^2 (Table 2) is taken as the effective ground Cs-137 surface concentration of the calibration site to be measured from the air and to be used to derive the airborne sensitivity coefficient (described in next chapter). The central Cs-137 concentration was measured to be 35.8 kBq/m^2.

Table 2: Measured Cs-137 concentration and weighted Cs-137 at various distances shown in Figure 8 from the calibration site at Beitostølen.

Sample no.	Distance (m)	Cs (kBq/m^2)	Weighted Cs (kBq/m^2)
0	0	35.8	0
1	8	37.4	0.63
2	32	51.3	2.59
3	64	42.0	2.54
4	128	27.1	1.06
5	8	31.7	0.53
6	32	29.4	1.49
7	64	58.2	3.51
8	128	36.5	1.42
9	8	35.0	0.59
10	32	35.7	1.80
11	64	36.0	2.17
12	128	37.5	1.46
13	8	37.3	0.63
14	32	42.3	2.14
15	64	37.1	2.24
16	128	23.8	0.93
17	8	32.6	0.55
18	32	37.4	1.89
19	64	43.7	2.63
20	128	25.5	1.00
21	8	33.9	0.57
22	32	38.8	1.96
23	64	33.3	2.01
24	128	21.4	0.84
Weighted sum of Cs concentrations			37.16

3.2 Re-processing of Cs data measured from helicopter

We observed that the standard way of stripping the overlapping low energy peaks in the Cs window due to U and Th and Compton continuum using the pad calibration data, does not yield a clean Cs-137 concentration especially in low Cs-137 concentration areas (Chapter 2.4, Figure 7). It rather shows the Cs-137 concentration distribution pattern very similar to either U, Th or total count due to presence of 609 keV line of Bi-214 (from decay chain of U) and 585 keV line of Tl-208 (from decay chain of Th) around the main energy line 662 keV of Cs-137 (see Figure 3). In the areas with high Cs-137 deposition, this low concentration pattern of insufficient stripping is not visible due to high Cs-137 deposition which we observed in Jotunheimen and Hattfjelldal area (Chapter 2.4, Figure 6) i.e. Cs deposition image was quite different than K, U and Th images (Baranwal et al., 2011). Oberlercher and Seiberl (1997) observed that low concentration of natural radioelements (i.e. K, U and Th) will increase the statistical error in determination of a Compton continuum

background when it is estimated by standard stripping method. They proposed a trapezoid method of determining the Compton continuum and stripping the Cs window data (see Figure 11).

New gamma-ray spectrometry calibration data were collected in 2015 by hovering the helicopter over the central point of calibration site (marked by a rectangle in Figure 4) at various heights ranging from ground level to 200 m. The measured count rates (cps) of Cs window were processed at each height in order to estimate their sensitivity coefficients for that height above the ground using weighted ground concentration of 37.16 kBq/m^2 at the calibration site described in Chapter 3.1.

Airborne spectrometer data were collected over a nearby water body at the same height intervals as over the calibration site. The average live time corrected counts over water were subtracted from average live time corrected counts collected over the calibration site at same height to remove background effects due to cosmic radiation, radiation from helicopter and radiation from radon in the air. Later, stripping corrections were applied to the background corrected data to calculate stripped U, Th and K window count rates using stripping coefficients calculated from measurements over calibration pads.

The processing steps were slightly modified during recalibration and reprocessing to follow Oberlercher and Seiberl (1997). Stripping corrections were applied to the background corrected data (live time, aircraft and cosmic corrections) to calculate stripped U, Th and K window count rates using stripping factors obtained from measurements on calibration pads (Stampolidis & Ofstad 2016). The Cs-137 window data (Cs^{ProcessedCounts} (equation 6) after live time, aircraft and cosmic correction) were further corrected using the spectral stripping method suggested by Oberlercher and Seiberl (1997) to remove contributions in the Cs-137 window due to K, U, Th and the Compton continuum. Figure 10 shows an average spectrum with a prominent Cs-137 peak (ca. 662 KeV) from 300 seconds measurement at ca. 68 m altitude from Beitostølen. Figure 11 shows a trapezoid area estimated using beginning and end channel of the Cs-137 window. A 10 points moving average filtered data from this trapezoid area was used as a model of the average background for Compton continuum. Cs-137 window count rates after stripping of the background and spectral overlapping due to U and Th were calculated using the following equation after Oberlercher and Seiberl (1997)

$$\mathrm{Cs^{corrected} = Cs^{ProcessedCounts} - Cs^{trapezoid} - 0.23U^{stripped} - 0.02Th^{stripped}} \quad (6),$$

where Cs^{corrected} were final Cs window count rates due to Cs-137 deposition only. Cs^{ProcessedCounts} were obtained after subtracting the background corrected Cs window counts over water body from processed Cs window counts over calibration site at the same height. U^{stripped} and Th^{stripped} were stripped U and Th window counts, respectively. The constants 0.23 and 0.02 represent the fraction of radiation from U and Th falling in the Cs-137 window (609 keV line of Bi-214 and 585 keV line of Tl-208).
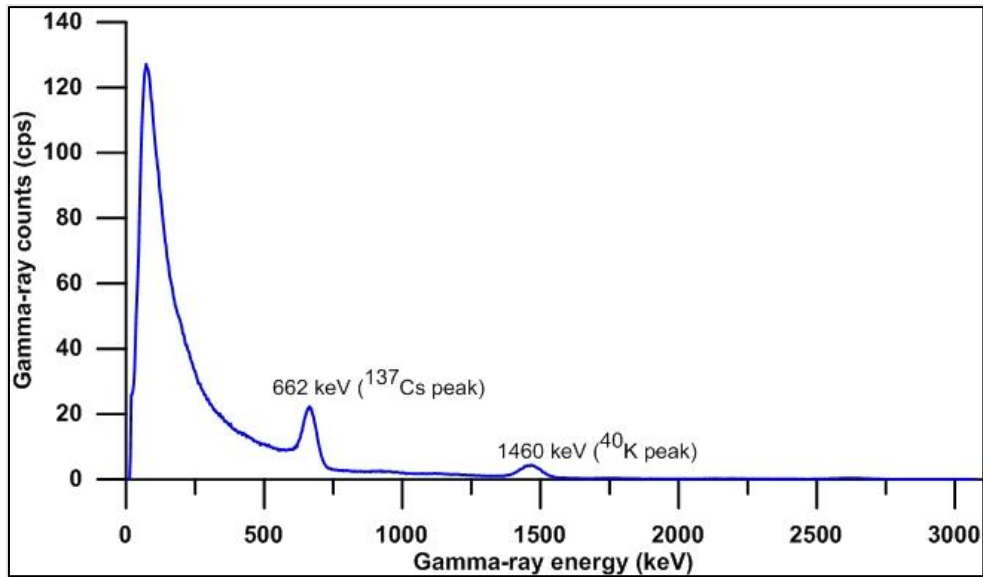
Figure 10: An average spectrum of gamma-rays from calibration site at Beitostølen.
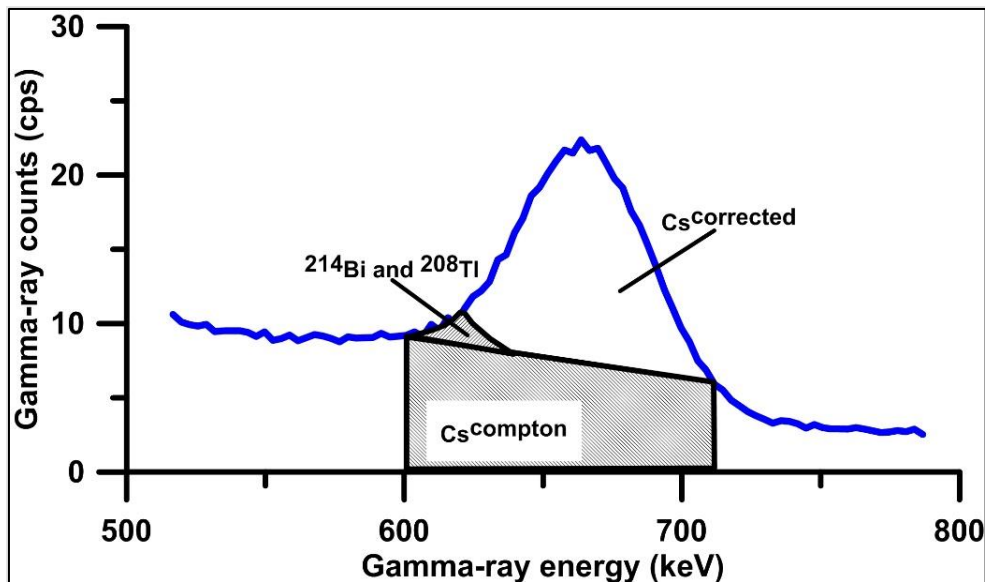
Figure 11: Zoomed averaged spectrum near Cs-137 peak showing the trapezoid area.

Later, $Cs^{corrected}$ were calculated at nominal altitude of 60 m using the height attenuation coefficient from Beitostølen data. From helicopter-borne recalibration data collected in 2015, we present final background, spectral and height corrected Cs-137 window count rates at the ground (with the helicopter situated on the ground) and at the nominal flying height of 60 m in Table 3.

Table 3: Cs-137 ground concentration (from hand-held measurements) and corrected Cs-137 window counts at the ground and at 60 m nominal height from helicopter-borne measurements at the calibration site Beitostølen.

Cs-137 ground concentration (kBq/m^2)	Corrected Cs-137 window counts (cps) from 2015
35.8 (at centre point)	878 (at the surface)
37.16 (weighted average)	280 (at 60 m height)

In the last step, sensitivity coefficients were calculated at the surface (S_1) and for the nominal height of 60 m (S_2) using values from Table 3 (dividing corrected Cs window count rates by respective Cs concentration) and shown in Table 4. Additionally, Cs sensitivity coefficient calculated by using the earlier approach from Baranwal et al. (2011) is also shown by S_3 for comparison. In the earlier approach, sensitivity coefficient calculated at the surface using a point source was height attenuated to the nominal flying height and then count rates measured at nominal height were divided by this sensitivity coefficient to calculate the Cs concentration. The Cs sensitivity surface coefficient (S_1) equal 24.53 (cps/kBq/m^2) yields 14.46 (cps/kBq/m^2) at 60 m height when using a height attenuation coefficient of 0.0088 per meter (Baranwal et al., 2011). The new calibration from Beitostølen show a correct sensitivity factor S_2 equal 7.53 (cps/kBq/m^2).

Table 4: Cs sensitivity coefficient estimated at surface and at nominal height from weighted ground concentration from the calibration site H1. Resulting Cs ground concentration using these three sensitivity coefficients are also shown.

New Cs sensitivities and ground concentrations	Estimated Cs sensitivity coefficients, (cps/kBq/m^2)		Estimated Cs ground concentration (kBq/m^2)	
At the ground (when helicopter landed)	S_1	24.53	C_1	35.80
Weighted average concentration and processed window counts at 60 m height	S_2	7.53	C_2	37.16
Same at 60 m nominal height using height attenuation coefficient equal 0.0088	S_3	14.46	C_3	19.36

Corresponding Cs concentrations calculated from these three sensitivities are shown by C_1 to C_3 in Table 4. The weighted average concentration (C_2) cannot be recovered by height attenuated sensitivity coefficient (S_3). Cs concentration (C_3) from height attenuated sensitivity (S_3) was underestimated by ca. 48 % with respect to weighted average ground concentration C_2. The new calibration at Beitostølen resulted in a correct height attenuation coefficient for Cs to be 0.018 per meter.

Based on this, reprocessing of spectrometry data for Cs-137 deposition from Jotunheimen and other areas were performed in following five steps:
1. Cs-137 window counts were corrected for lifetime and cosmic radiation
2. Stripping was applied to U and Th window counts
3. Compton background was removed from Cs window following Oberlercher and Seiberl (1997) and equation (6)
4. Compton corrected Cs-137 window was height attenuated to a nominal height (e.g. 60 m) using the attenuation coefficient 0.018 per meter.
5. Height attenuated Cs window data were converted to ground Cs-137 deposition using sensitivity coefficient S_2.

3.3 Effect of reprocessing of spectrometry data for Cs-137 ground deposition

In this chapter, we demonstrate efficiency of the new processing strategy using examples from Drangedal (Stampolidis and Ofstad 2015) and Jotunheimen (Baranwal et al. 2011) data. Drangedal is low in Cs-137 deposition, however, Jotunheimen is high in Cs-137 deposition.

3.3.1 Drangedal area

Figures 12a and 12b show the ground Cs-137 concentration using traditional window processing (left) and new processing using recalibration and the Oberlercher & Seiberl (1997) method (right). For both images, we applied the traditional Cs-137 sensitivity factor (S_3) from the point source calibration. The average Cs-137 ground concentration is here reduced to about half and the influence from natural radioisotopes (U, Th and K) is minimised. The spectral trapezoid processing described by Oberlercher and Seiberl (1997) works well in removing the pattern of natural isotopes in the Cs-137 calculation to a large extent. Applying the new Cs sensitivity factor (S_2) from the Beitostølen calibration, the Cs-137 concentration will increase with a factor of 1.8 - 2.0 but the Cs-137 distribution pattern will be the same.
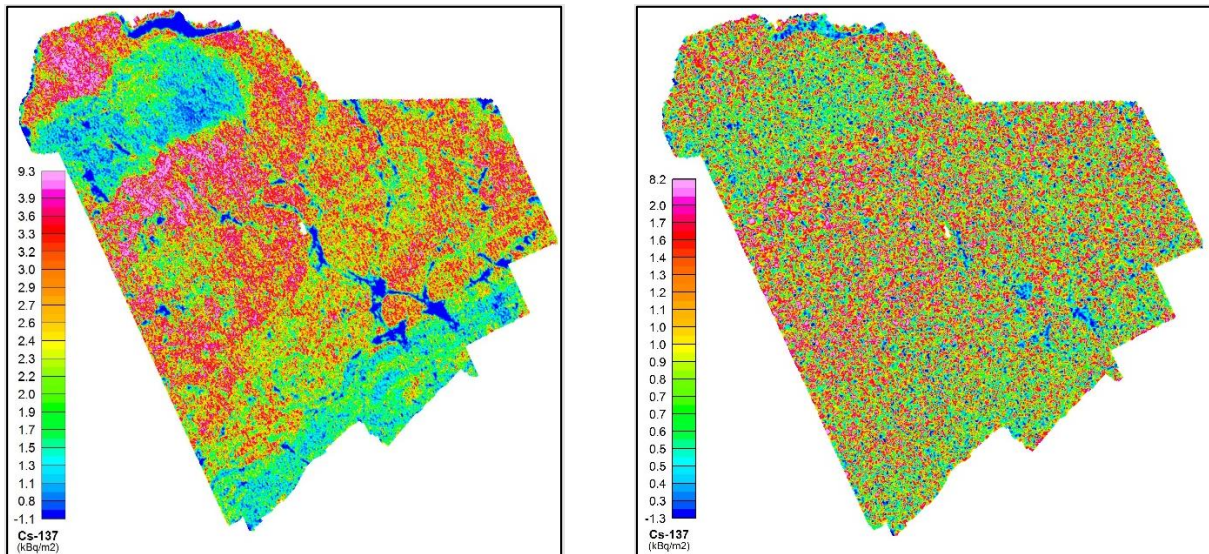
Figure 12: Drangedal ground Cs-137 concentration. From traditional window processing (same data as in Figure 7, left) and from new spectrum processing using old sensitivity factor (right).

3.3.2 Jotunheimen area

The corrected Cs window counts ($Cs^{corrected}$) are calculated using equation (6) for all 2011 Jotunheimen data. $Cs^{corrected}$ was height attenuated to a nominal height of 60 m and finally a new surface activity for Cs-137 was calculated dividing the height attenuated $Cs^{corrected}$ by the new sensitivity coefficient (S_2).

The final recalculated ground concentration of Cs from the helicopter-borne survey is decay corrected to 1st June 2011 and shown in Figure 13 as a grid of 200 m. The Cs-137 distribution is the same as that originally processed by Baranwal et al. (2011)

(Figure 4) but the average Cs-137 ground concentration is increased by a factor of ca. 1.6.

Figure 13 illustrates that the Cs-137 deposition in the area was heterogeneous, with activity ranging from <1 to 114 kBq/m^2 (grid values). The most contaminated area is situated around a mountain plateau between the lake Vinstre and the valley Heimdalen, where the highest activity value from the helicopter-borne spectrometer readings reached 133 kBq/m^2. This corresponds to a value of about 240 kBq/m^2 in spring 1986, when about 130 kBq/m^2 of Cs-134 was also present (based on a Cs-134/Cs-137 ratio of 0.56 (De Cort et al. 1998)).

Figure 13: Cs-137 deposition in 2011 (decay corrected to 1st June 2011) obtained from new reprocessing. Water bodies are replaced with dummy values (blank/white regions within the grid). Blank area in the north west is showing absence of the data over parts of Jotunheimen highland park. Water bodies are also overlaid in the image in semi-transparent light blue colour. Circles show in situ measurements and soil sample locations between 2001 to 2016 by DSA. Triangles mark location of calibration sites in 2011 for hand-held spectrometer used in in-situ measurements in 2012 and 2016. Rectangle marks location of recalibration site in 2015 for helicopter-borne recalibration survey.

3.4 Comparing ground-based measurements and reprocessed aerial data for Cs-137 from Jotunheimen

Figure 14 shows comparison of Cs concentrations in samples (from 2011 and 2012) presented in Figure 5 with reprocessed 2011 Jotunheimen data (extracted from the grid in Figure 13). Figure 15 shows a comparison of all the soil samples and in situ measurements collected during 2001 to 2016 (ca. 50 locations).
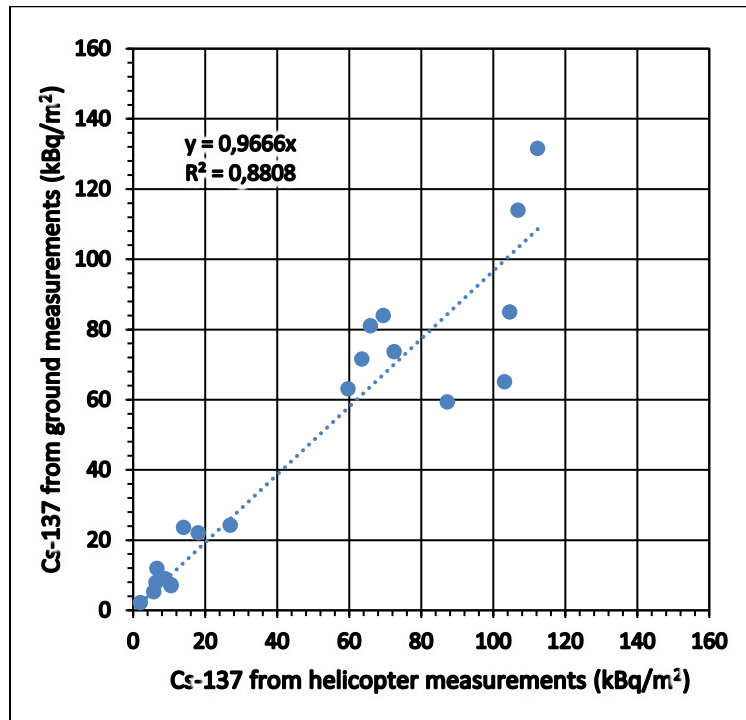
Figure 14: Cs-137 concentrations from the reprocessed helicopter-borne survey data vs. ground measurements and soil analyses (2011-2012) in Jotunheimen (data from Thørring et al. 2019).
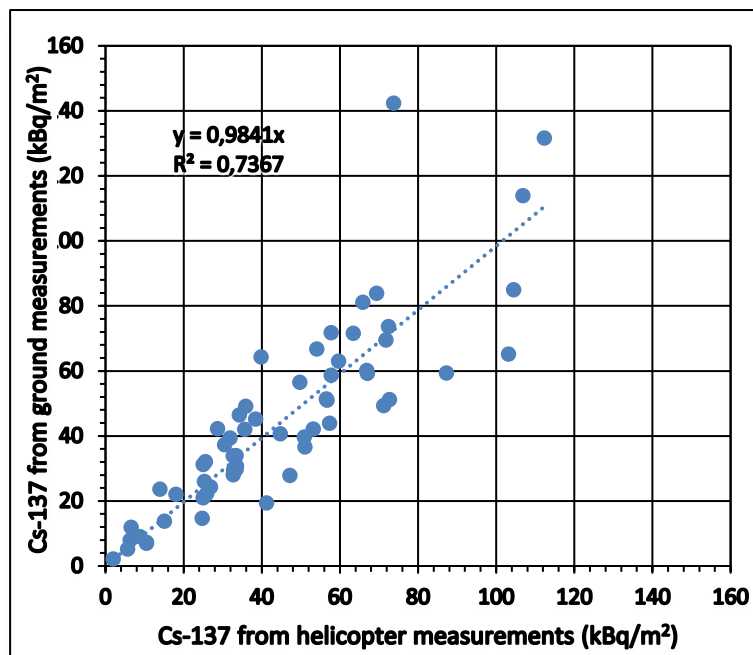
Figure 15: Cs-137 concentrations from the reprocessed helicopter-borne survey data vs. ground measurements and soil analyses (2001-2016) in Jotunheimen (data from Thørring et al. 2019).

All the deposition values shown here are decay corrected to 1st June 2011 (the year of the aerial survey). The in-situ measurements (ground measurements and soil samples) were taken over a 15 years period (for Figure 15) presuming that there has been no significant run-off of Cs-137. This is supported by an early study in the watershed of lake Øvre Heimdalsvatn which indicated that just 0.01-0.1 % of the deposited activity was removed by surface runoff in 1989 (Thørring et al. 2019).

We see that the coefficient in the regression model is almost 1 for all the locations which is very good considering the variabilities that exist in the field, e.g. soil density, humidity, small and large spatial scales and the number of samples. It is also important to note that the aerial survey and the various ground measurements are using different analytical procedures and were conducted at different times. Furthermore, the footprints are very different i.e. 120 m X 150 m for helicopter-borne data and about 1 m^2 for the ground measurements. While the aerial survey results show Cs-137 deposition levels ranging from <1 to 133 kBq/m^2, the maximum levels observed during the *in-situ* measurements in 2011-2016 reached almost 1 MBq/m^2.

4. Cs-137 DEPOSITION MAPS FROM DIFFERENT PARTS OF NORWAY

AGRS data relevant to this Cs mapping work has been collected from different parts of Norway between 1987 and 2015. During the years of intensive airborne data acquisition (2011-2015), NGU has collected several individual surveys in North and South Norway. Some of these are adjacent to each other and can be stitched together to give a continuous image of the Cs deposition. In this chapter the stitching procedure and reprocessing of the data are presented from different areas in Mid and North Norway.

4.1 Data recovery and Stitching strategy

The gamma-ray spectrometry data were collected by different spectrometers in different file formats by NGU and other suppliers during 1987-2015. Table 5 describes the NGU equipment and format of the gamma ray spectrometry data files.

Table 5: Specification of the NGU gamma ray spectrometers used by NGU at different times after the Chernobyl accident in 1986.

Time period	Spectrometer model	No. of channels	Crystal type and volume	File format
1987 - 1993	Geometrics GR-800	256	NaI, 4 x 4 l	LOD
1994 - 1998	Geometrics GR-820	256	NaI, 4 x 4 l + 1 X 4 l	LOD
1998 - 2009	Geometrics GR-820	256	NaI, 4 x 4 l + 1 X 4 l	HUM
2010 - 2015	Radiation Solutions RSX-5	1024	NaI, 4 x 4 l + 1 X 4 l	RSI

LOD and HUM files are binary files and they are converted to ascii format to get access to the whole gamma ray spectrum which is needed for the reprocessing. The old data saved in LOD files were not converted in ASCII format for full spectra rather it was converted in ASCII format for only window counts for K, U and Th. Janusz Koziel from NGU could retrieve full spectra from LOD files by decoding the binary LOD files to an ascii format. This was a time-consuming process since the binary formats were

changed from one year to another. A proper calibration strategy was not followed in the early years. Therefore, we did not have all the calibration coefficients needed to do a proper calculation of Cs-137 deposition from such areas. For these areas, we reprocessed the airborne data using available calibration coefficients from that year or near years (e.g. background correction, stripping and height attenuation (Baranwal et al. 2011)). Individual Cs-137 ground deposition from each survey area were decay corrected to 26th April 2016 (30th anniversary of Chernobyl nuclear accident i.e. also half-life of Cs-137) using equation (7).

$$N(t) = N_0 e^{-lt} \qquad\qquad\qquad (7),$$

where *N(t)* is deposition at a time *t*, N_0 is initial deposition, $l = \ln(2)/T_{1/2}$, $T_{1/2}$ is half-life which is 30.17 years (11018.3 days) for Cs-137.

The resulting Cs-137 depositions were compared between adjacent overlapping survey areas and a regression analysis was performed to calculate slope and intercept of the correlation. The slope and intercept were used to level Cs-137 deposition from one of the areas to match with level of Cs-137 from other survey area assuming it as a base (e.g. Frosta data in 2015, Stampolidis & Ofstad 2016). Finally, levelled Cs-137 deposition grids are stitched (or mosaiced) with Cs-137 deposition grids of adjacent survey areas.

Details of the individual survey will be given under each area presented in the next chapters. The helicopter-borne gamma-ray spectrometry surveys were carried out mostly using a spectrometer of 16 litres downward-looking crystals, and sometimes an additional 4 litres upward-looking with accumulation time one second. Fixed-wing surveys normally uses the double crystal volume and double speed (≈ 200 km/h), but half (0.5 second) accumulation time for each record. Average flying altitude varied between 60 to 200 m depending on the local topography and helicopter-borne or fixed-wing survey. An accumulation time of one second for each helicopter-borne and 0.5 second for fixed-wing surveys provided enough gamma-ray counts at a sampling interval of ca. 30 m. About 70 % of the counts are generally assumed to originate from an oval of width twice the flying height and length twice the flying height and the distance travelled during the counting time, i.e., roughly 120 m and 150 m, respectively for the helicopter-borne survey. For the fixed-wing surveys, the flying altitude varies and the footprint (measured area) varies accordingly.

In general, Cs-137 deposition grids from different surveys can be stitched together using a static trend removal and suture method available by the GridKnit module in Geosoft's Oasis Montaj (Geosoft 2018). This method works fine when final deposition is calculated using appropriate calibration coefficients and there are good overlapping areas. It does not matter if the data is collected by different spectrometers in different years. However, it cannot work well when deposition or concentration is not calculated by following proper calibration steps and data is presented by only count rates. We experienced that trend removal method even using slope method did not work well in such situations. For these cases, we stitched grids in by calculating a slope and intercept ourselves from overlapping areas of the grids to be stitched together (Baranwal 2016, Dumais 2014).

 All Cs deposition maps presented in this chapter are produced using the new calibration and processing procedure described in Chapter 3.2.

4.2 Cs deposition from Jotunheimen, Vågå and Otta

A new Cs deposition map from the Jotunheimen area is compiled from two adjacent helicopter-borne gamma ray surveys. Specifications for these surveys are given in Table 6. The outline of the two areas are shown in Figure 16. Because both surveys were collected by NGU using RSX-5 spectrometer and properly processed using all the appropriate calibration parameters, there was not a big mismatch in the level of Cs-137 at the boundary of these two surveys after reprocessing as described in Chapter 3.2. Various calibration coefficients were same as reported in original processing reports (Baranwal et al. 2011, Ofstad 2015) except sensitivity coefficient S_2 was used to calculate the Cs-137 ground deposition. Cs-137 ground deposition from both the surveys were decay corrected to 26th April 2016 (using equation 7). Both surveys were stitched together using static trend removal under GridKnit function in Geosoft's Oasis Montaj (Geosoft 2018). Resulting stitched grid is shown in histogram equalisation and linear scales in Figures 17 and 18, respectively. Histogram equalisation scale highlights all the areas even with smaller changes and it is good for geological mapping and to see where Cs-137 is relatively higher. However, this presentation can lead to a wrong interpretation of a rather larger area showing a greater deposition. The linear scale is better to look for highest and lowest deposition areas therefore Cs-137 map from Jotunheimen and surroundings are presented in both histogram and linear scales versions.

The Cs ground concentration in this area is well above the noise level (see Discussion).

Table 6: Specification of the NGU gamma ray spectrometer surveys in the Jotunheimen and Otta – Vågå areas.

Survey area	Survey year	Spectrometer	Line spacing (m)	*Average measuring height (m)	Reference
Jotunheimen	2011	RSX-5	1000	65	Baranwal et al. 2011
Otta - Vågå	2015	RSX-5	200	83	Ofstad 2015

* Targeted altitude was 60 m.
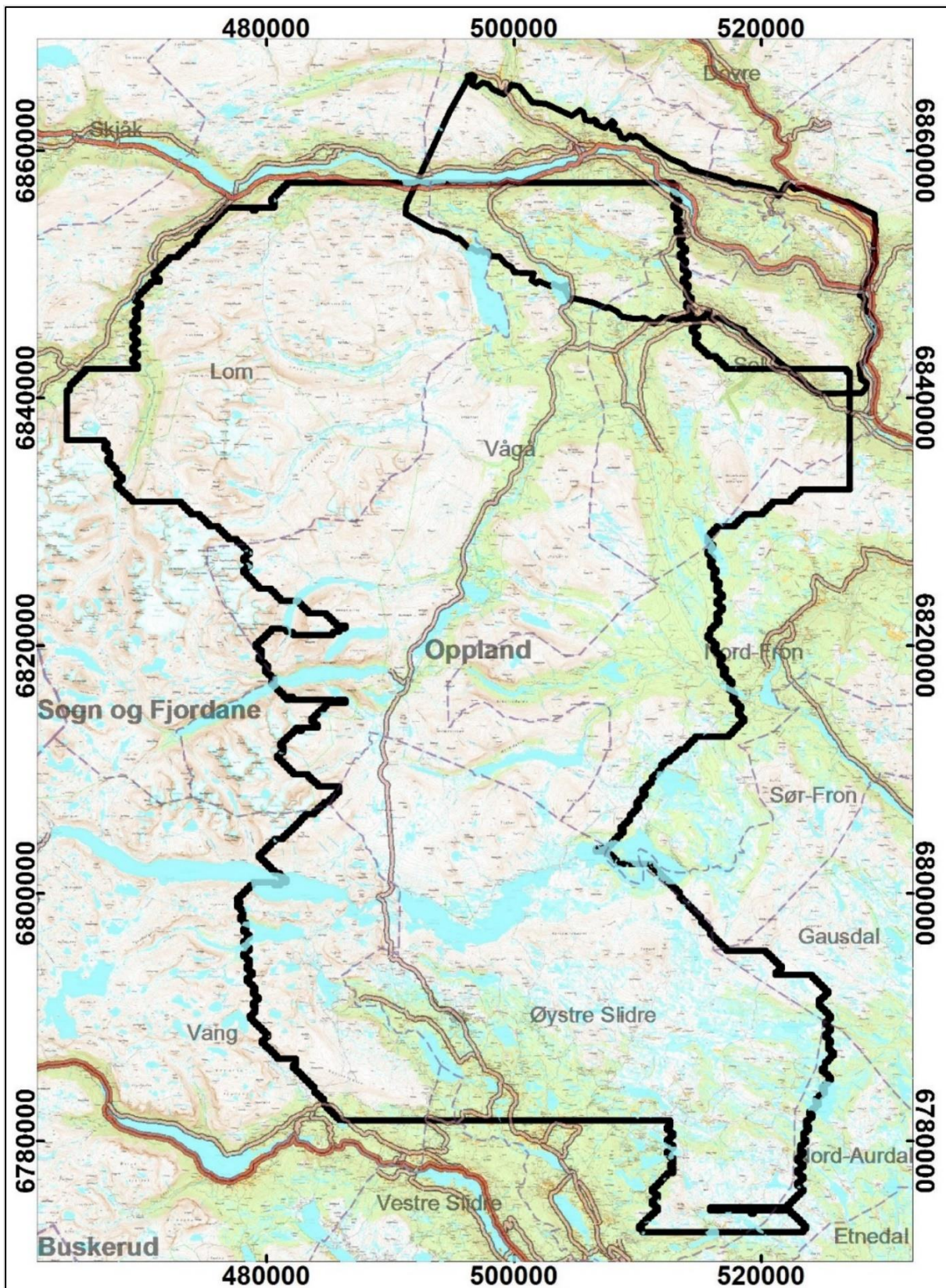
Figure 16: Outline of the Jotunheimen-Otta-Vågå surveys are shown by thick black lines.
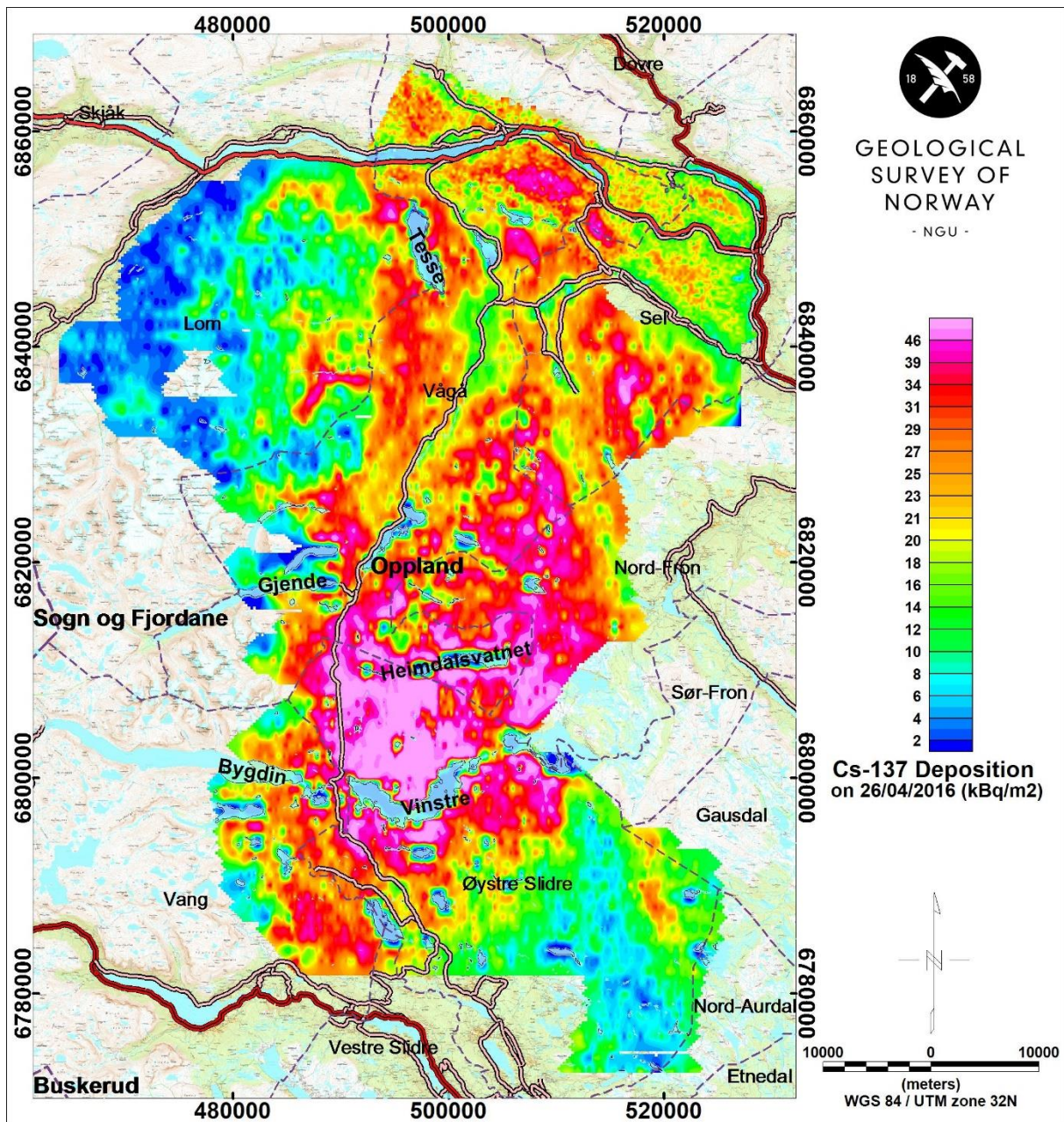
Figure 17: Stitched Cs-137 ground concentration for the area Jotunheimen – Otta – Vågå in histogram equalisation scale. Water bodies are also overlaid in the image in semi-transparent light blue colour.
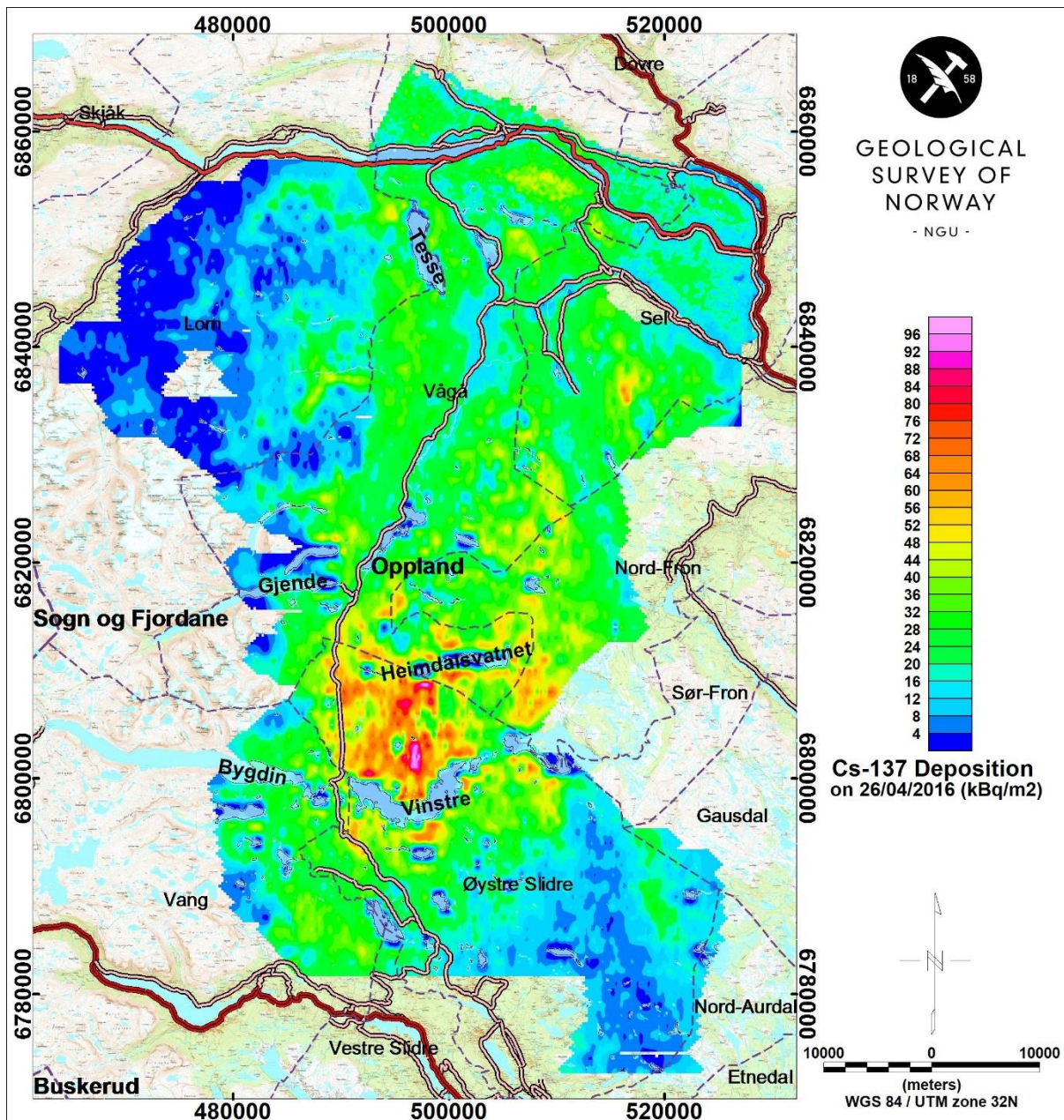
Figure 18: Stitched Cs-137 ground concentration for the area Jotunheimen – Otta – Vågå in linear scale. Water bodies are also overlaid in the image in semi-transparent light blue colour.

4.3 Cs deposition from Trøndelag

Various helicopter-borne and fixed-wing surveys were performed in Trøndelag area after 1986 (Table 7, Figure19). Many areas were surveyed by NGU using helicopter during 1988 to 1999. A fixed-wing survey named TRAS-12 (Trøndelag Airborne Survey 2012) was performed in 2012 to 2013. Recently (in 2015), new surveys were carried out in Trøndelag south of Trondheim and at Steinkjer. In addition, a few flight lines were measured at Frosta-Fosen to get overlapping survey areas between TRAS-12 and older helicopter-borne surveys. The airborne data from an area which overlaps with two regions (Trøndelag and TRAS-12) made stitching of radiometry data possible from both areas as they were collected by different survey companies and spectrometers. Details of all the surveys in Trøndelag are summarised in Table 7.

Table 7: Specification of the NGU gamma ray spectrometer surveys in Trøndelag region.

Survey name	Survey year	Spectrometer	Line spacing (m)	*Average measuring height (m)	Reference
Grong	1988-1989	GR-800	250 m	82 m	Mogaard et al. 1989 Rønning et al. 1990
Andorsjøen	1990	GR-800	200 m	88 m	Rønning 1991
Snåsavatnet	1990-1991	GR-800	200 m	86 m	Rønning 1992a, 1992b, 1992c
Meråker	1991	GR-800	200 m	75 m	Mogaard & Blokkum 1993
Stiklestad	1991	GR-800	200 m	79 m	Rønning 1995a
Fosen	1992	GR-800	200 m	85 m	Rønning 1995b
Vuku	1992	GR-800	100 m	75 m	Skilbrei 1994
Oppdal	1993	GR-800	100 m	64 m	Mogaard 1993
Røyrvik	1993-1994	GR-800	100, 200, 400 m	75 m	Rønning 1995c
Skorovatn	1993-1994	GR-800	100, 200, 400 m	82 m	Rønning 1995c
Røros	1999	GR-820	200 m	78 m	Beard & Mogaard 1999
TRAS	2012-2013	RSX-5	250 m	195 m	Novatem 2014a
Trøndelag	2015	RSX-5	200 m	83 m	Rodionov et al. 2016
Steinkjer Frosta	2015	RSX-5	250 m	87 m	Stampolidis & Ofstad 2016

* Targeted altitude was 60 m.

Outlines of all the survey areas for Trøndelag region except Oppdal (Table 7) are shown in Figure 19. Oppdal survey did not overlap with other survey areas and it is situated further south. Therefore, it is presented in a separate chapter. Black boundary surveys were performed by helicopter during 1988-1999. Green boundary represents TRAS-12 fixed-wing survey and red boundary shows helicopter-borne surveys in 2015.
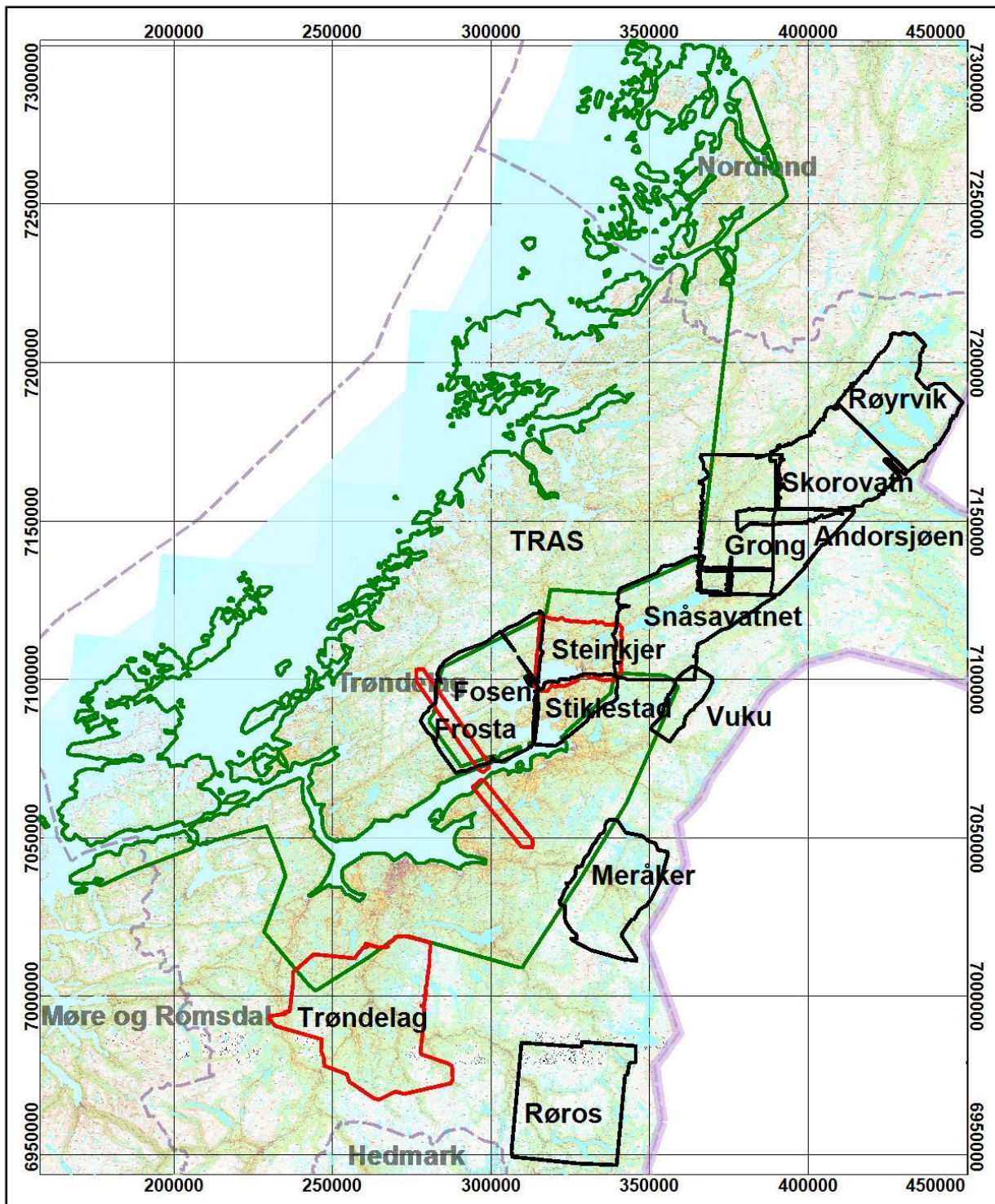
Figure 19: Outline of the helicopter-borne and fixed-wing surveys in Trøndelag region from 1988-2015. Black boundary surveys were performed by helicopter during 1988-1999. Green boundary represents TRAS-12 fixed-wing survey during 2012-2013 and red boundary shows helicopter-borne surveys in 2015.

Targeted drape height was 60 m for all the airborne surveys. Helicopter could manage to fly an average altitude between 64 to 88 m in Trøndelag region (data from above 120 m flying were discarded). However, fixed-wing aircraft from Novatem (TRAS-12 survey) could not drape-fly the mountainous terrain as good and lots of data were collected at higher altitude i.e. > 200 m. Therefore, all the data flown above 240 m height at STP were set as 240 m, in order to avoid unrealistic high concentrations due to height corrections (IAEA, 1991). Gridded altitude values for TRAS-12 data is shown

in Figure 20. This gave average flying altitude as 195 m (without STP correction) for TRAS-12 data.
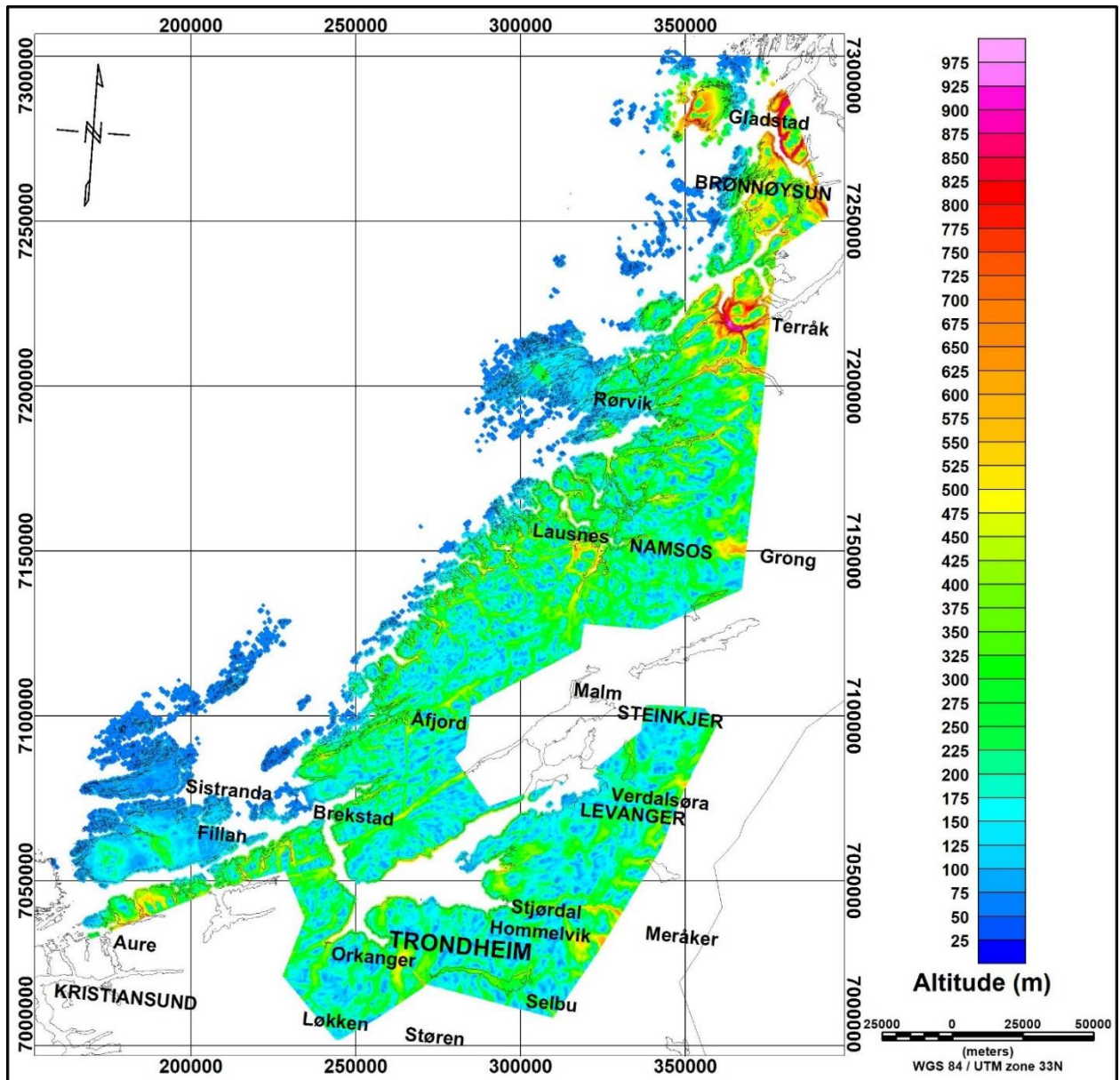
Figure 20: Altitude of the flight and spectrometer for fixed-wing TRAS survey by Novatem.

4.3.1 Reprocessing of Trøndelag data

Old data were not processed properly using required calibration coefficients as described in Baranwal et al. (2011) and IAEA (1991). There were also lots of irregularities in radar altimeter and GPS recordings. These were manually inspected and corrected. Full spectra were recovered from LOD files and subsequently reprocessed following the steps described in Chapter 3.2. Background correction, stripping and height attenuation coefficients were used from Walker (1992) for surveys measured within 1988 to 1992 (Grong, Andorsjøen, Meråker, Snåsavatnet, Stiklestad, Fosen and Vuku). However, stripping coefficients from Walker & Smethurst (1993) were applied to Oppdal and Røyrvik surveys. Background, cosmic correction, stripping and height attenuation coefficients from Rønning et al. (2002) were applied to

Skorovatn and Røros surveys. A sensitivity coefficient of 25 counts/sec/(kBq/m^2) was applied to all old data to calculate ground deposition of Cs-137 (Walker & Smethurst 1993). Finally, individual Cs-137 ground deposition from each survey area was decay corrected to 26th April 2016 using equation (7).

TRAS-12 data (Novatem 2014a) were reprocessed using background, cosmic correction, stripping and height attenuation coefficients from Novatem (2014b) and following the reprocessing steps described in Chapter 3.2. Two different sensitivity coefficients were used for two different aircrafts collecting the TRAS-12 data as 14.8 and 13.3 for PA31_C_GJDD and PA31_C_FWNG, respectively. The sensitivity values for two different aircrafts were calculated from Novatem's intermediate and final processed spectrometry data delivered to NGU. We did not use sensitivity value of 9.1 as mentioned in Novatem's calibration report (Novatem 2014b) because this sensitivity value did not reproduce the Cs-137 deposition grid delivered by Novatem. Finally, Cs-137 ground deposition were decay corrected to 26th April 2016 using equation (7). Cs-137 from TRAS-12 survey was very patchy, therefore, a 100 m Butterworth low-pass filter was applied to smooth the data.

General processing for Trøndelag, Frosta and Steinkjer data was described in Rodionov et al. (2016) and Stampolidis & Ofstad (2016). Background, cosmic correction, stripping and height attenuation coefficients were used from these reports following the reprocessing steps described in Chapter 3.2. Sensitivity coefficient S$_2$ was used to calculate Cs-137 ground deposition. Finally, Cs-137 ground deposition was calculated for 26th April 2016 using half-life decay equation (equation 7).

4.3.2 Stitching of Cs-137 ground deposition from Trøndelag except Oppdal

Stitching of old surveys (1988-1999) with new surveys (2012-2015) was a very challenging task because the Cs-137 deposition values were changing from one survey to another. All the Cs-137 deposition values calculated for 26th April 2016 from Trøndelag region (Figure 19) were stitched together making Trøndelag and Steinkjer as the base grid. Helicopter-borne survey by NGU in Frosta in 2015 overlapped with 2012-2013 fixed-wing TRAS-12 survey and 1992 helicopter-borne survey in Fosen. Therefore, Frosta data was used to level Cs-137 deposition from Fosen and TRAS-12 to bring them at the level of Frosta.

First, Cs-137 ground deposition (calculated for 26th April 2016) from Trøndelag, Frosta and Steinkjer surveys in 2015 were merged using Geosoft's mosaic tool. Overlapping areas between mosaiced grids from 2015 and reprocessed grid from TRAS-12 survey were extracted and a regression analysis was performed as described by Baranwal (2016) and Dumais (2014). Linear regression of Cs-137 deposition from overlapping areas between these two regions (Frosta by helicopter-borne survey in 2015 and TRAS-12 by fixed-wing survey) resulted in a relation Y=4.7X where Y is C-137 from overlapping mosaiced data and X is C-137 from overlapping TRAS-12 survey. Therefore, TRAS-12 data was multiplied with 4.7 and stitched together with mosaiced Cs-137 from 2015 surveys removing a static trend (a fixed value) from the TRAS-12 data. This resulted in *stitched_new_data* for Cs-137 for surveys from 2012 to 2015 in Trøndelag region.

Second, all the old data from Trøndelag were stitched together. Fosen, Stiklestad, Snåsavatnet, Vuku, Grong and Andorsjøen had almost similar level of Cs-137 deposition. Therefore, they were stitched together one by one starting with Fosen and removing a static trend from the other grid. Røyrvik and Skorovatn had similar levels of Cs-137 therefore they were stitched together removing the static trend. Regression analysis between a stitched Fosen and other grids and a stitched Røyrvik and Skorovatn grids resulted in a relation Y=0.63X-0.5, where Y is stitched Fosen and other grids and X is stitched Røyrvik and Skorovatn grid. The stitched Røyrvik and Skorovatn grid was leveled with regression parameters and stitched with Røros, Meråker and the stitched Fosen and other grids resulting in *stitched_old_data* for Cs-137 for surveys from 1988 to 1999 in Trøndelag region.

A regression analysis between overlapping areas of the 1992 Fosen survey and 2015 Frosta lines resulted in a relation Y=0.9X+1.3, where Y is Frosta Cs-137 and X is Fosen Cs-137. Therefore, *stitched_old_data* was modified using these regression parameters and stitched together with *stitched_new_data* using static trend removal to yield final stitched data for all the surveys from 1988 to 2015 in Trøndelag region. The stitched grid is shown in two colour scales as histogram equalisation and linear in Figures 21 and 22, respectively. We can see that there is not much level difference at various survey boundaries in both the images. Trøndelag area shows Cs-137 deposition at several places but its intensity is not as strong as in Jotunheimen. Aerial measurements show maximum Cs-137 deposition of ca. 40 kBq/m^2 in Trøndelag i.e. ca. 1/3rd of the deposition in Jotunheimen.

The Cs ground concentration in the Trøndelag area is partly well above the noise level (see Discussion).
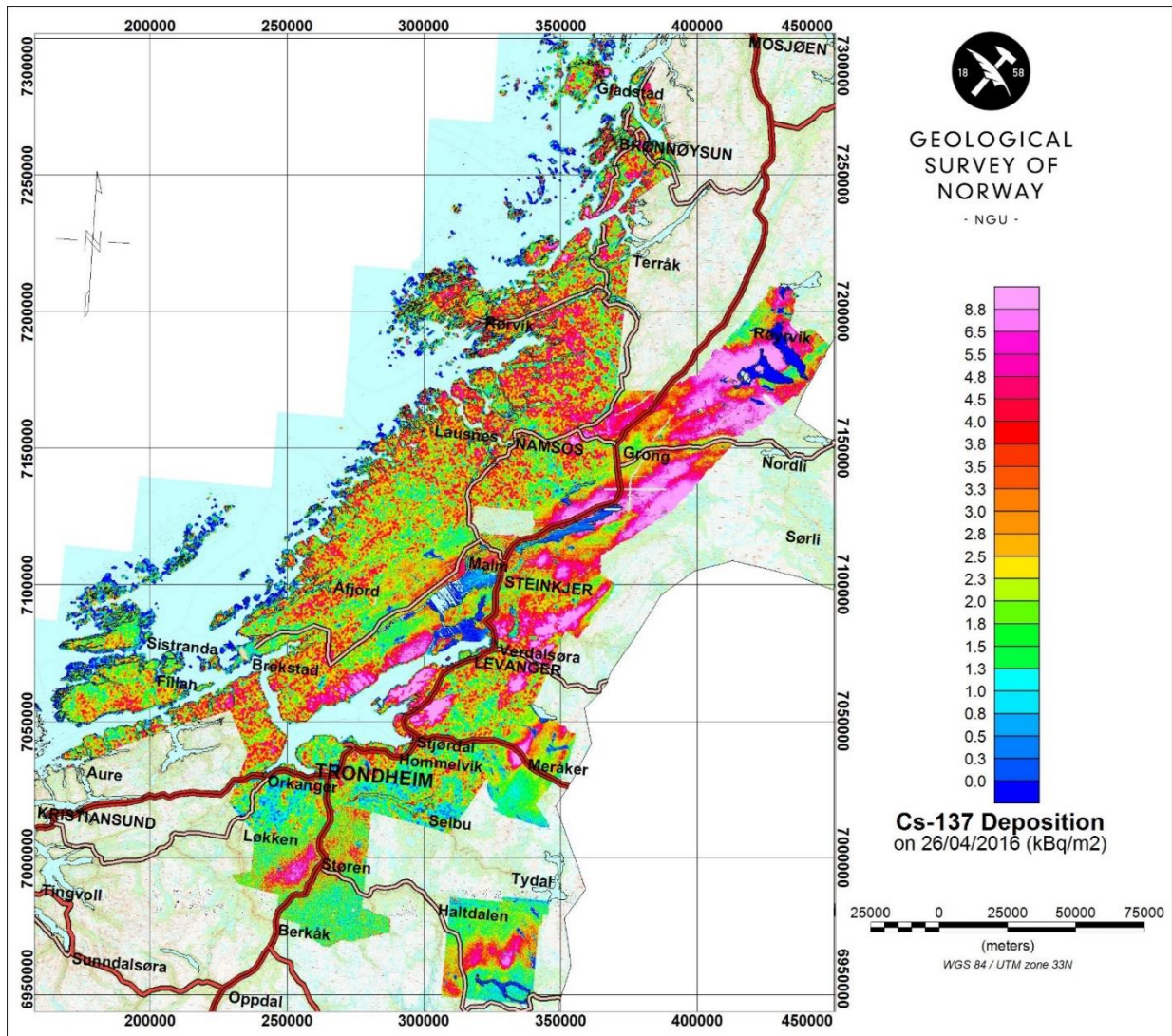
Figure 21: Stitched grid (histogram equalisation scale) of Cs-137 ground deposition on 26th April 2016 from Trøndelag region.
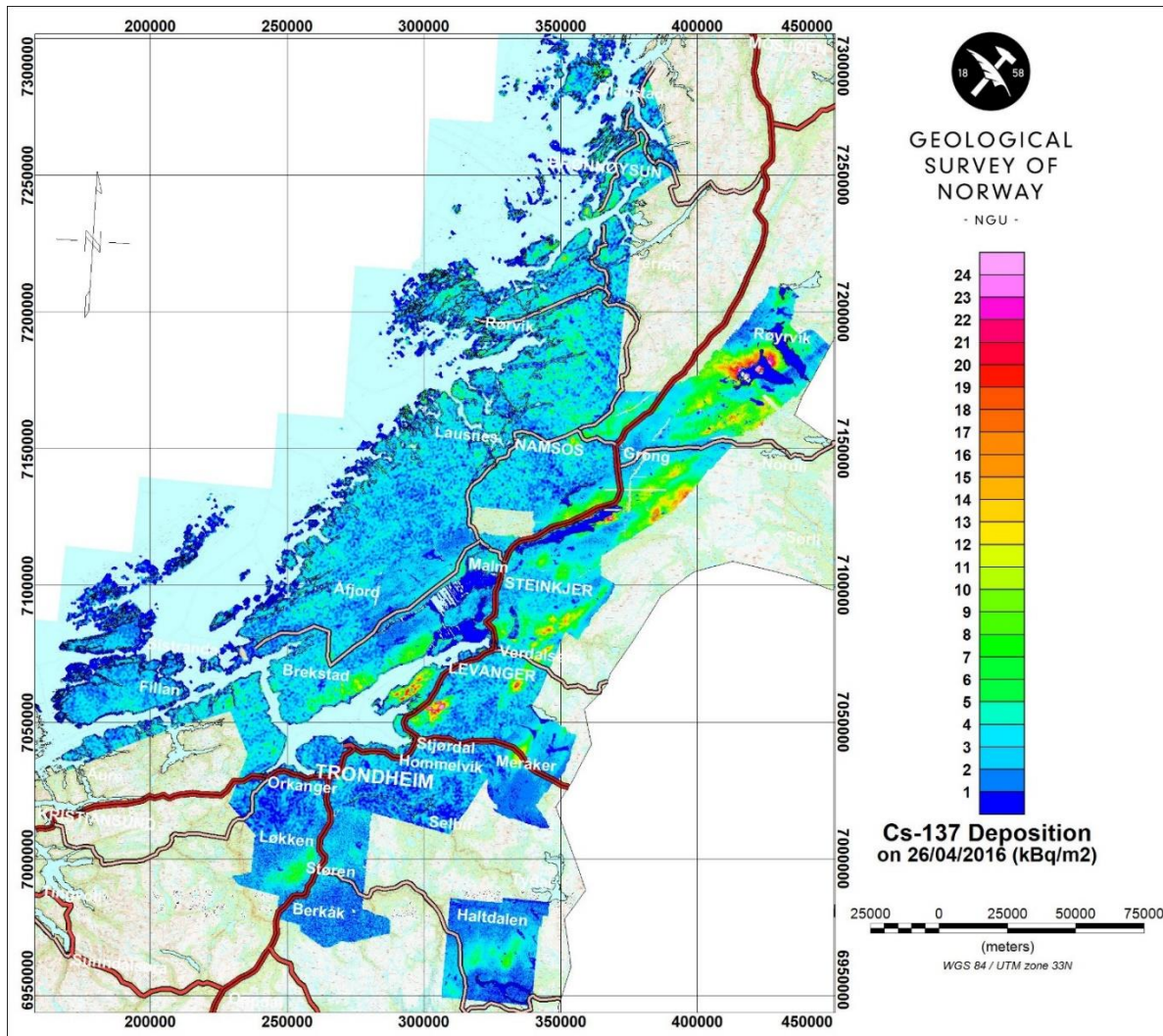
Figure 22: Stitched grid (linear scale) of Cs-137 ground deposition on 26th April 2016 from Trøndelag region.

4.3.3 Cs-137 ground deposition from Oppdal

Oppdal area was surveyed by NGU using a helicopter in 1993. Oppdal is far from rest of the survey areas in Trøndelag (Figure 19). Therefore, it is presented separately. Processing of Oppdal data was done in the same way as it was done for other old data from Trøndelag region (e.g. Fosen). The Cs-137 deposition data was calculated to 26th April 2016 using half-life decay equation (7) and the relation $Y=0.9X+1.3$ is used (assuming X for Oppdal's Cs-137 deposition level from the actual survey) to match with the level of recent helicopter-borne survey deposition (Frosta in 2015). Deposition of Cs-137 in Oppdal is shown in histogram and linear scales in Figures 23 and 24, respectively. We observe much less Cs-137 in Oppdal, ca. 10 kBq/m^2 at some places and even lesser at other places. Cs-137 deposition of 5 kBq/m^2 is considered as the noise in Cs-137 calculation because we could remove most of Bi-214 and Compton scattering from Cs-137 window but slight effect from it still remain. Later, we observe that new processing shows ca. 5 kBq/m^2 Cs-137 concentration from the areas where no Cs-137 peak was observed in the spectrometry data e.g. Høgtuva, Hollandsfjord, Rana and Hellemobotn.

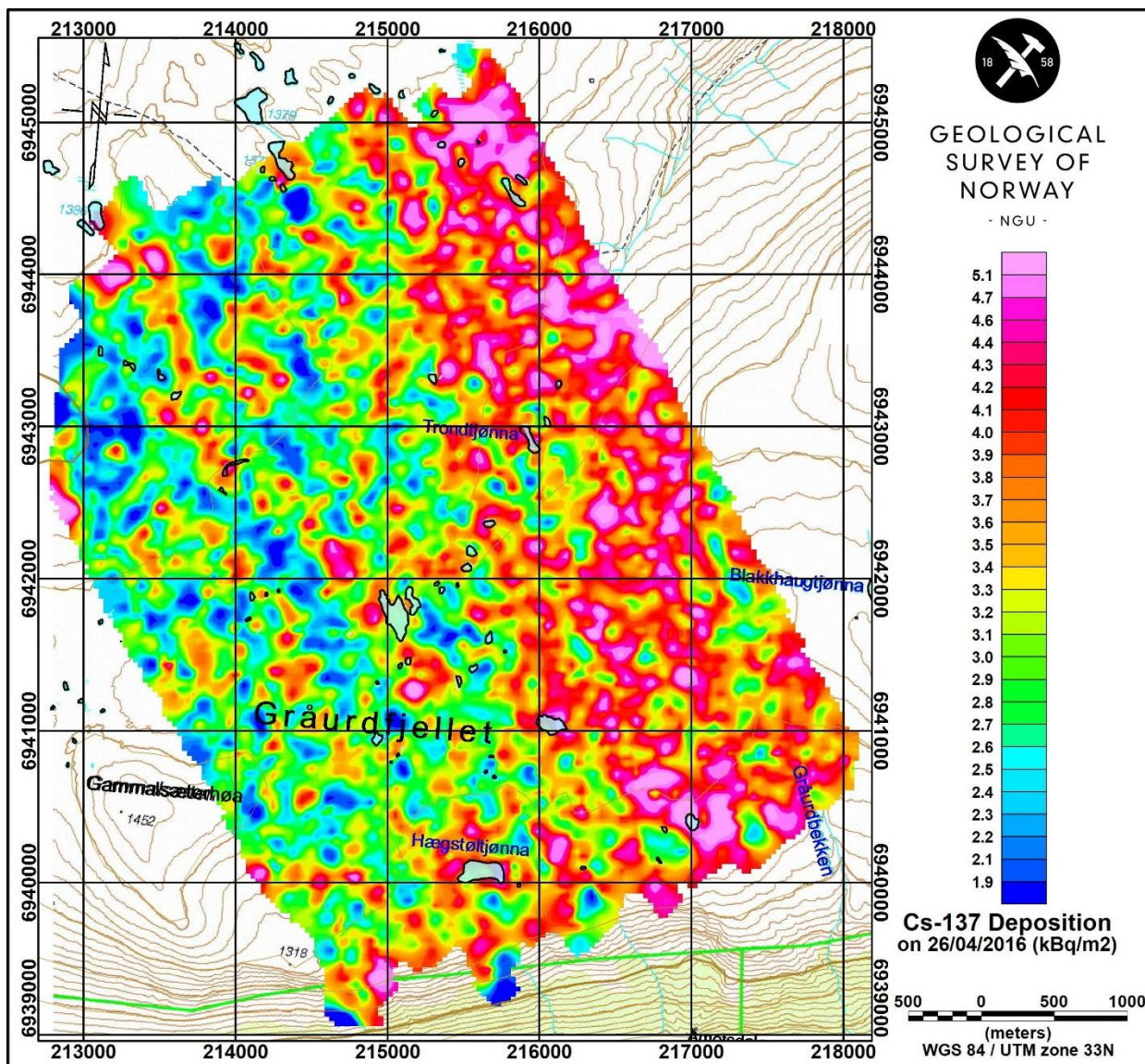Figure 23: Cs-137 ground deposition in histogram equalisation scale from the Oppdal area.
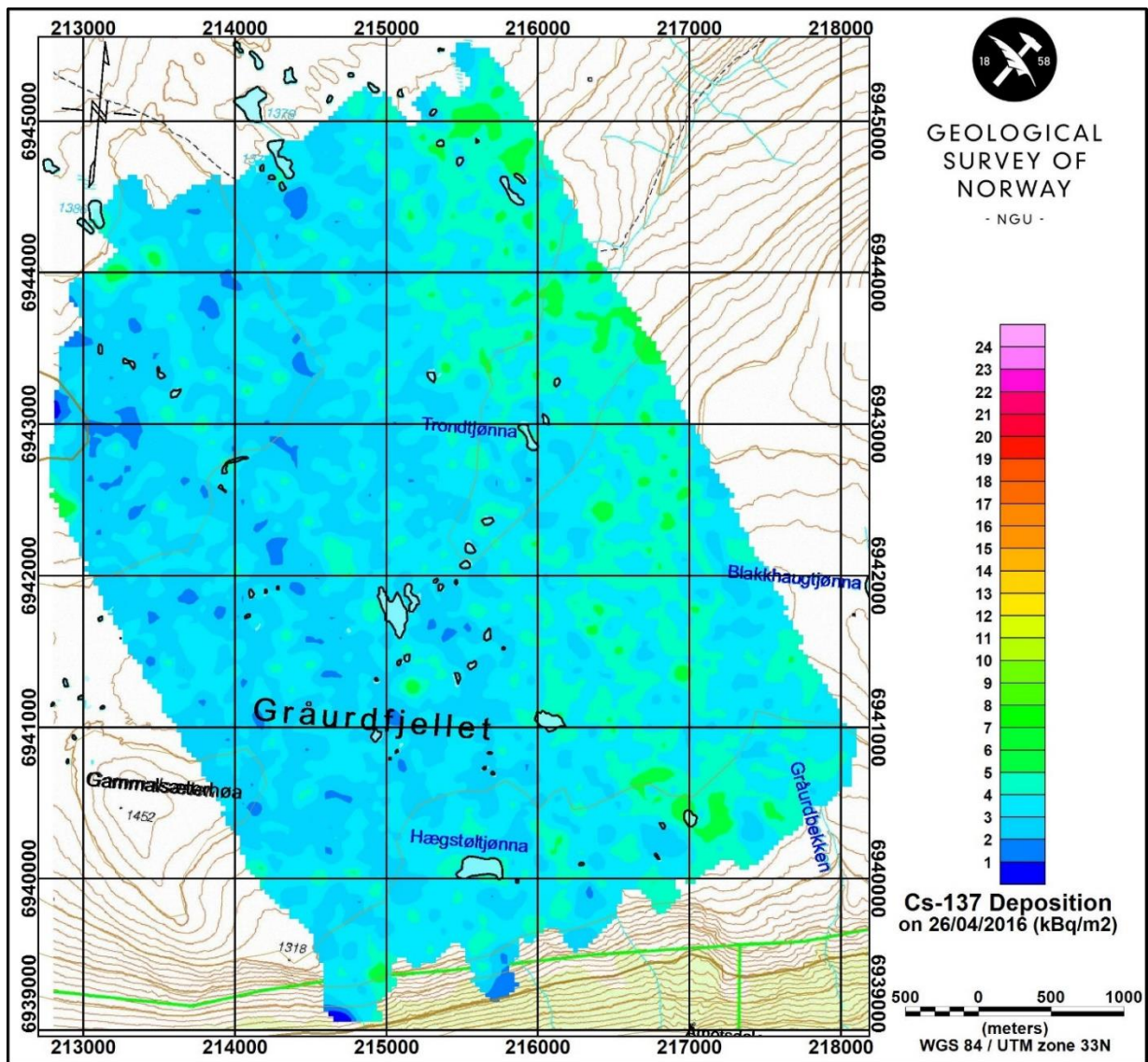
Figure 24: Cs-137 ground deposition in histogram equalisation scale from the Oppdal area.

4.4 Cs deposition from Nordland

NGU has performed helicopter-borne surveys in various regions of Nordland county during 1987 to 2014. Survey area names and survey specifications are mentioned in Table 8 and shown in a map in Figure 25. There were lots of irregularity in radar altimeter and GPS recordings in surveys before 2010. These were manually inspected and corrected. Full spectra were recovered from the LOD files and then they were reprocessed following the steps described in Chapter 3.2. Background correction, stripping and height attenuation coefficients were used from Walker (1992) for surveys from 1987 to 1992 (Mo i Rana, Høgtuva and Hellemobotn). However, stripping coefficients from Walker and Smethurst (1993) were applied to Røssvatnet, Korgen and Hjartfjellet surveys. A sensitivity coefficient of 25 counts/sec/(kBq/m^2) was applied to these old data before 2010 to calculate ground deposition of Cs-137. Finally, individual Cs-137 ground deposition from each survey area were decay corrected to 26th April 2016 using equation (7).

Spectrometry data in Nordland were collected with similar system and processed in same way as for Trøndelag. Therefore, we used the same equation of Fosen Y=0.9X+1.3 to level the data from Nordland which were collected with GR-800 before 2010 to match with Cs-137 deposition as on 26th April 2016 from new surveys. Korgen and Hjartfjellet (collected using GR-820) were treated in the same manner as Skorovatn in Tøndelag. Spectrometry data collected in 2012-2014 (Rana, Holandsfjord and Hattfjelldal) were processed with the new processing method described in Chapter 3.2 and applying the new sensitivity factor S$_2$.

Table 8: Specification of the NGU gamma ray spectrometer survey in Nordland, Norway.

Survey area	Survey year	Instrument	Line spacing (m)	*Average measuring height (m)	Reference
Hattfjelldal	2014	RSX-5	200	86	Rodionov et al. 2014
Røssvatnet,	1993	GR-800	200	80	Mogaard & Olesen 1997
Korgen, Hjartfjellet	1994 1995	GR-820	200	71 86	Mogaard & Olesen 1997
Rana	2012	RSX-5	100	87	Rodionov et al. 2012
Høgtuva	1987	GR-800	200	84	Mogaard et al. 1988
Holandsfjord	2013	RSX-5	200	87	Rodionov et al. 2013
Hellemobotn	1991	GR-800	200	80	Mogaard 1992

* Targeted altitude was 60 m.
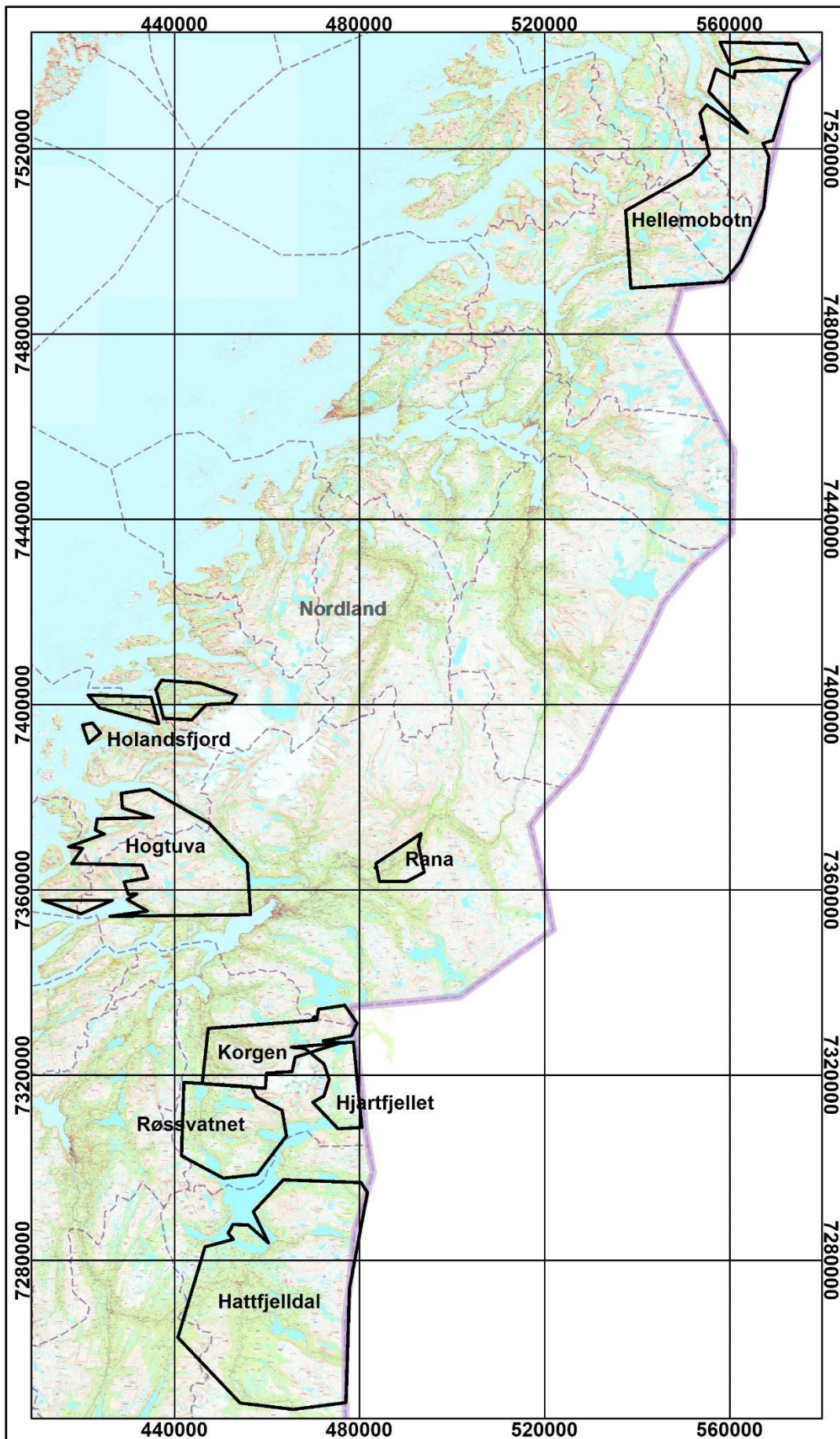
Figure 25: Helicopter-borne survey boundaries for different survey areas in Nordland.

4.4.1 Cs deposition from Hattfjelldal

Hattfjelldal area was surveyed during MINN project in 2014 by helicopter using NGUs RSX-5 instrument. General processing of spectrometry data and maps for K, U and Th were presented in an NGU report by Rodionov et al. (2014). Airborne survey boundaries are shown in Figure 25. Specifications for the survey are given in Table 8. Cs-137 deposition map from the Hattfjelldal area produced by the new reprocessing is shown in Figures 26 and 27 with both colour scale histogram equalisation and linear scales, respectively. Hattfjelldal has shown similar level of Cs-137 as seen in Jotunheimen. The Cs ground concentration in Hattfjelldal is well above the noise level (see Discussion).

Figure 26: Cs-137 ground deposition in histogram equalisation scale from the Hattfjelldal area.
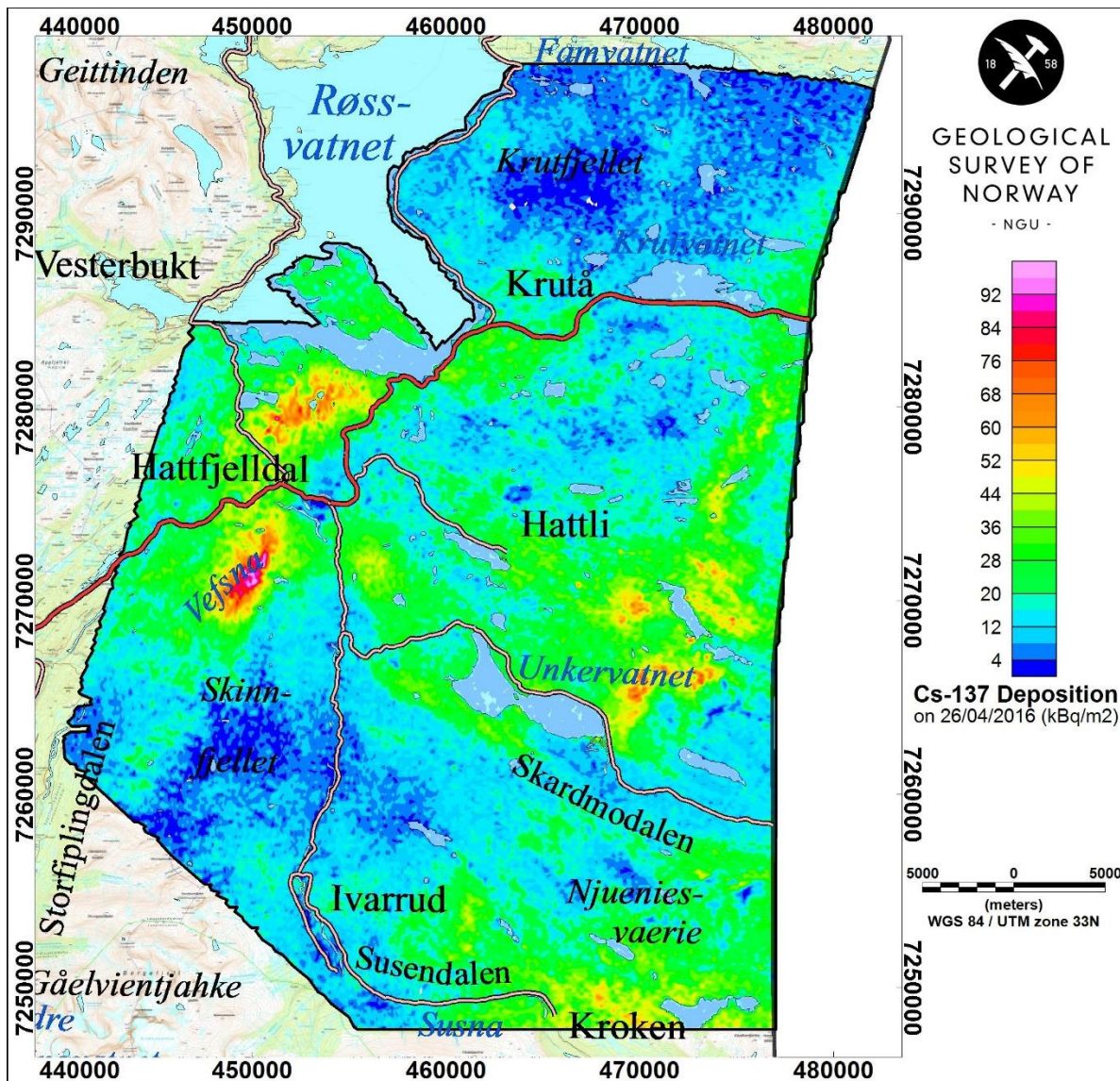
Figure 27: Cs-137 ground deposition in linear scale from the Hattfjelldal area.

4.4.2 Cs-137 deposition from Røssvatnet, Hjartfjellet and Korgen

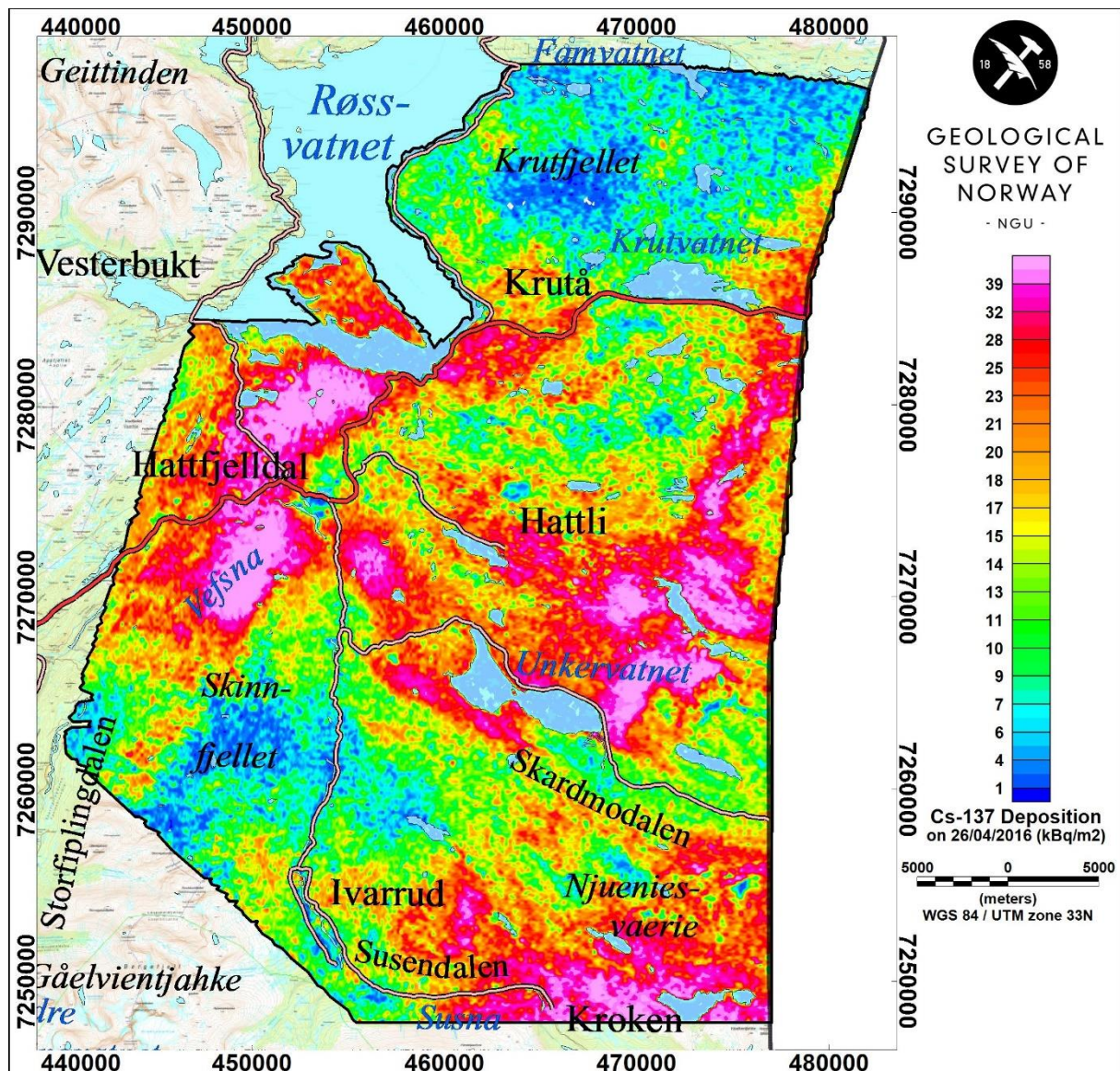Røssvatnet, Hjartfjellet and Korgen were surveyed by NGU during 1993-1995 using GR-800 and GR-820 spectrometers (Table 8). An initial processing of spectrometry data was documented in an NGU report by Mogaard & Olesen (1997). Airborne survey outline is shown in Figure 25. Specifications for the survey are given in Table 8. Airborne spectrometry data for these three areas are reprocessed individually as described in Chapter 3.2. After reprocessing, we observed along-line noise in the data which was micro-levelled. Cs-137 from Korgen and Hjartfjellet (surveys from 1994 and 1995, respectively using GR-820) were levelled using the expression Y=0.63*X-0.5 to match with Røssvatnet level (survey from 1993 using GR-800) and then stitched together with Røssvatnet by removing a static trend from later two grids. Finally, the resulting stitched grid from Røssvatnet, Korgen and Hjartfjellet was levelled to match with the level of Cs-137 deposition obtained from more recent surveys (e.g. Frosta from 2015) using the expression Y=0.9X+1.3.

Final levelled Cs-137 deposition grid from the Røssvatnet, Korgen and Hjartfjellet area is shown in Figures 28 and 29 in histogram equalisation and linear scales, respectively. It does not show much of Cs-137 in this area like Jotunheimen and Hattfjelldal. Although, there are some areas with slight high Cs-137 deposition in the range of ca. 10 kBq/m^2. The noise level is assumed to 5 kBq/m^2 because we did not observe any Cs-137 peak in the areas where Cs-137 concentration was calculated ca. 5 kBq/m^2.

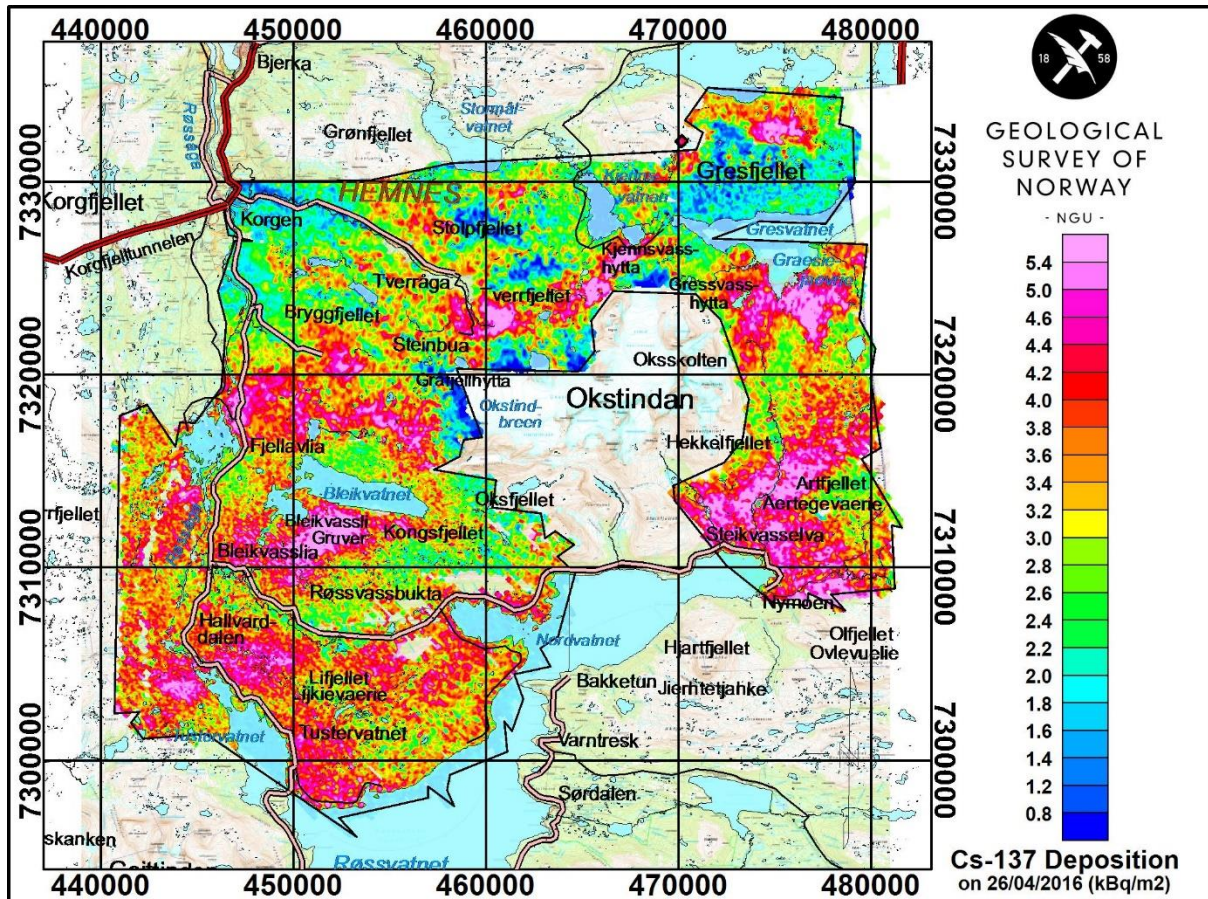Figure 28: Cs-137 ground deposition in histogram scale from the Røssvatnet, Korgen and Hjartfjellet area.
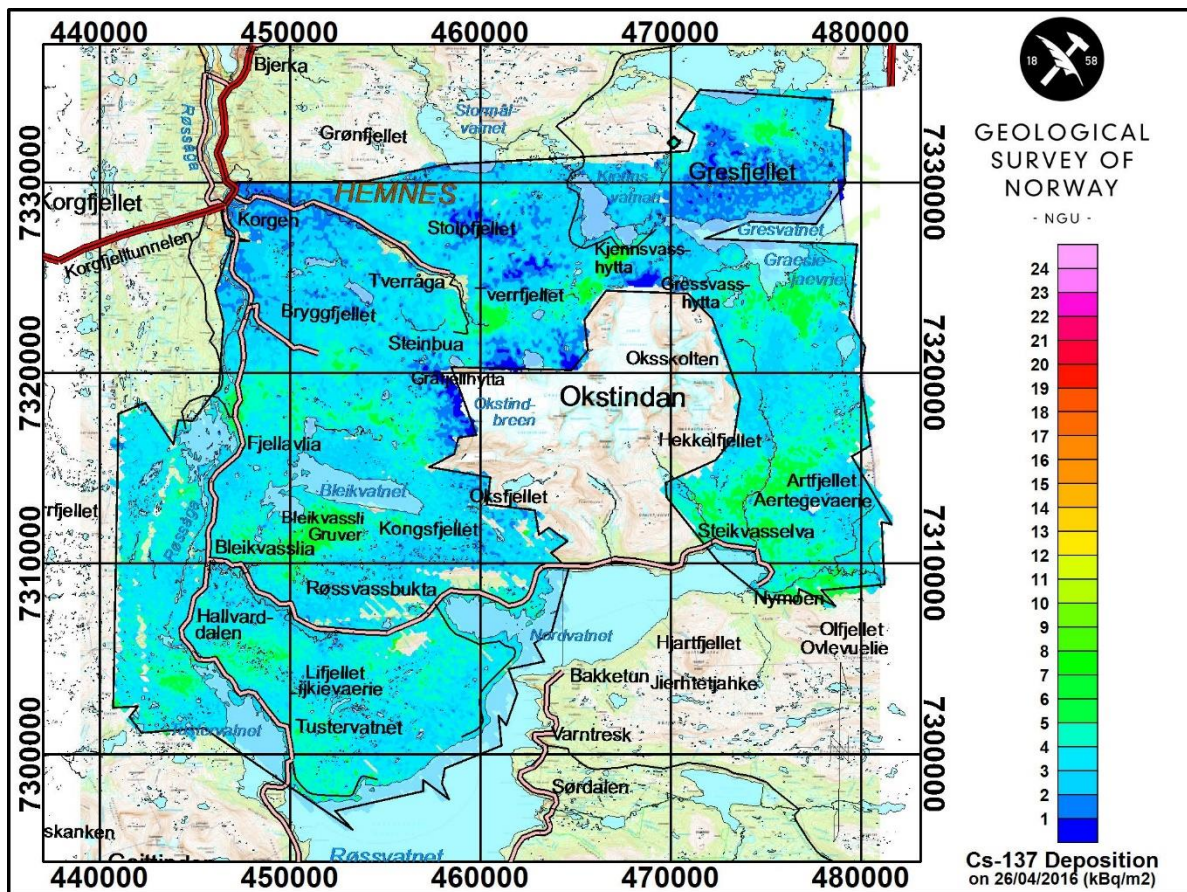
Figure 29: Cs-137 ground deposition in linear scale from the Røssvatnet, Korgen and Hjartfjellet area.

4.4.3 Cs-137 deposition from Høgtuva

Høgtuva was surveyed by NGU (Table 8) in 1987 using GR-800 spectrometer. A rough processing of spectrometry data was documented in an NGU report by Mogaard et al. (1988). Airborne survey boundary is shown in Figure 25. Specifications for the survey are given in Table 8. Reprocessing of Høgtuva data was done according to the processing strategy described for old data in Chapter 3.2. Cs-137 deposition grid calculated for 26th April 2016 was levelled to match with the level of Cs-137 deposition obtained from recent surveys (e.g. Frosta flights from 2015) using the expression $Y=0.9X+1.3$.

Levelled Cs-137 deposition map from the Høgtuva area produced after reprocessing and levelling is shown in Figures 30 and 31 applying histogram equalisation and linear colour scales, respectively. Høgtuva shows Cs-137 in the area below 5 kBq/m^2 which is below the noise level. A close inspection of the spectrometry data reveals that there was no Cs-137 peak present in the Høgtuva data.

Figure 30: Cs-137 ground deposition in histogram scale from the Høgtuva area.

Figure 31: Cs-137 ground deposition in linear scale from the Høgtuva area.

4.4.4 Cs-137 deposition from Rana

Rana area was surveyed by helicopter during the MINN project in 2012 using NGUs RSX-5 instrument. General processing of spectrometry data and maps for K, U and Th was presented in an NGU report by Rodionov et al. (2012). Airborne survey outline is shown in Figure 25. Specifications for the survey are given in Table 8. Cs-137 deposition map from the Rana area produced after reprocessing as described in Chapter 3.2 is shown in Figures 32 and 33 in histogram equalisation and linear colour scales, respectively. Rana shows Cs-137 deposition below 5 kBq/m^2 which is below the noise level. A close inspection of the spectrometry data reveals that there was no Cs-137 peak present in the Rana data.

Figure 32: Cs-137 ground deposition in histogram equalisation scale from the Rana area.

Figure 33: Cs-137 ground deposition in linear scale from the Rana area.

4.4.5 Cs-137 deposition from Holandsfjord

Holandsfjord area was surveyed in 2013 during the MINN project using helicopter and NGUs RSX-5 instrument. General processing of spectrometry data and maps for K, U and Th was presented in an NGU report by Rodionov et al. (2013). Airborne survey outline is shown in Figure 25. Specifications for the survey are given in Table 8. Cs-137 deposition map from the Holandsfjord area produced after reprocessing as described in Chapter 3.2 is shown in Figures 34 and 35 in histogram equalisation and linear colour scales, respectively. Holandsfjord shows Cs-137 deposition below 5 kBq/m^2 which is below the noise level. A close inspection of the spectrometry data reveals that there was no Cs-137 peak present in the Holandsfjord data.
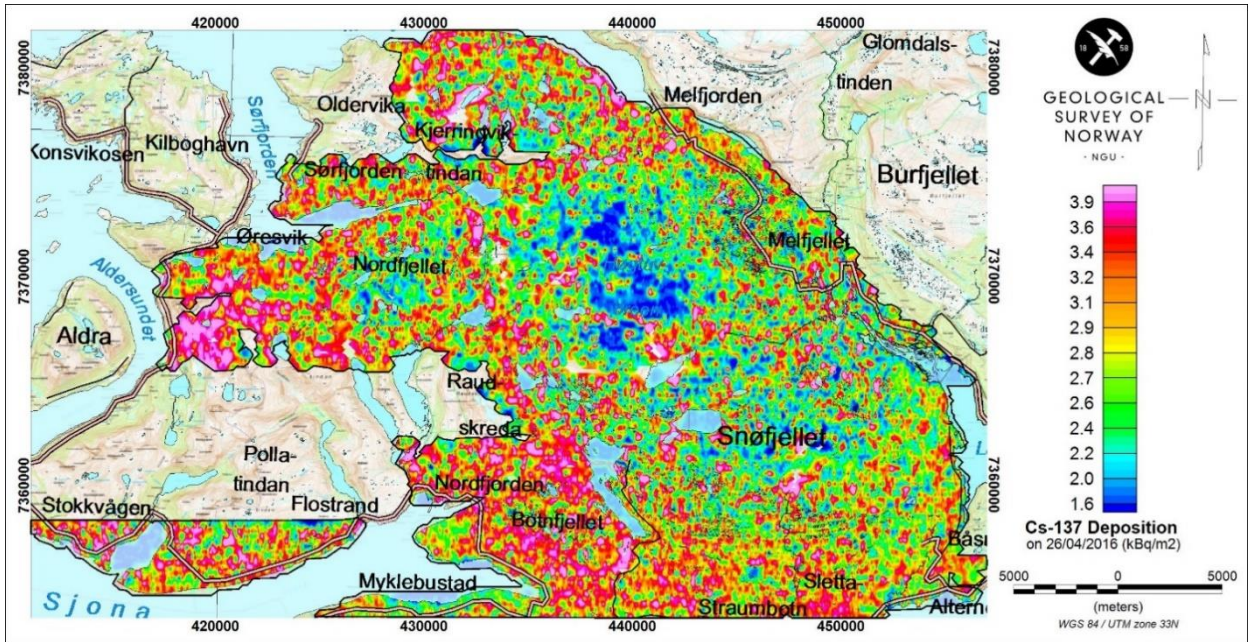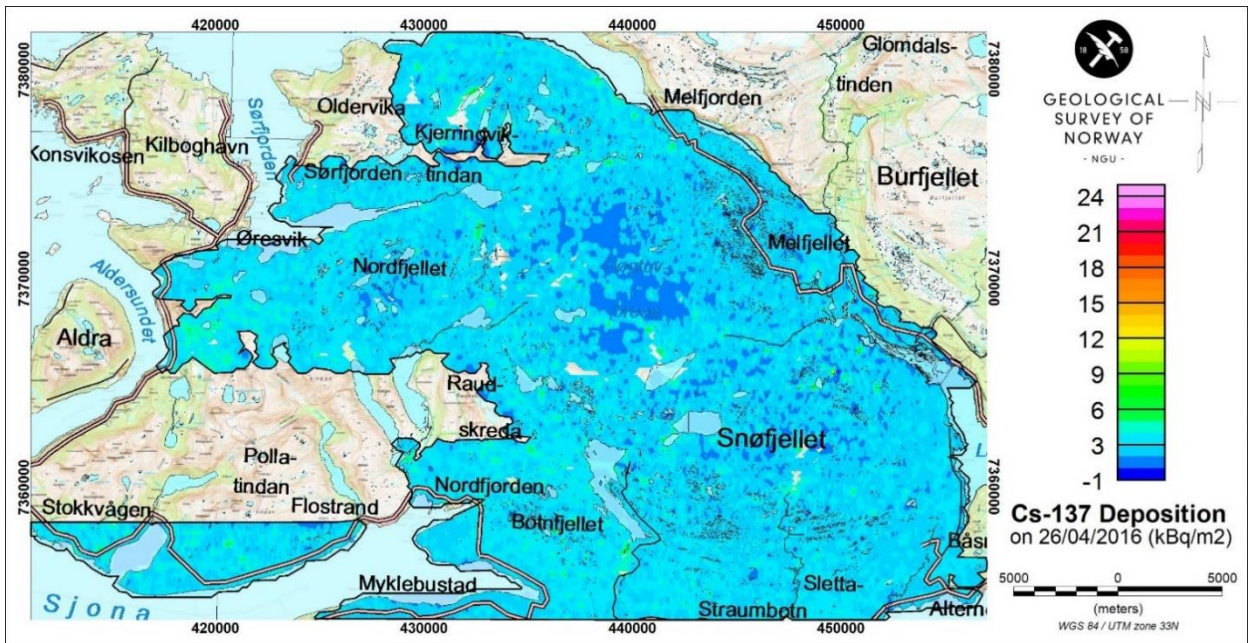

Figure 34: Cs-137 ground deposition in histogram equalisation scale from the Holandsfjord area.

Figure 35: Cs-137 ground deposition in linear scale from the Holandsfjord area.

4.4.6 Cs deposition from Hellemobotn

Hellemobotn was surveyed by NGU in 1991 (Table 8) using GR-800 spectrometer. A rough processing of spectrometry data was documented in an NGU report by Mogaard (1992). Airborne survey outline is shown in Figure 25. Specifications for the survey are given in Table 8. Cs-137 deposition map from the Hellemobotn area produced after reprocessing and levelling is shown in Figures 36 and 37 in histogram equalisation and linear colour scales, respectively. Hellemobotn shows Cs-137 concentration below 5 kBq/m^2 which is below the noise level. A close inspection of the spectrometry data reveals that there was no Cs-137 peak present in the Hellemobotn data.
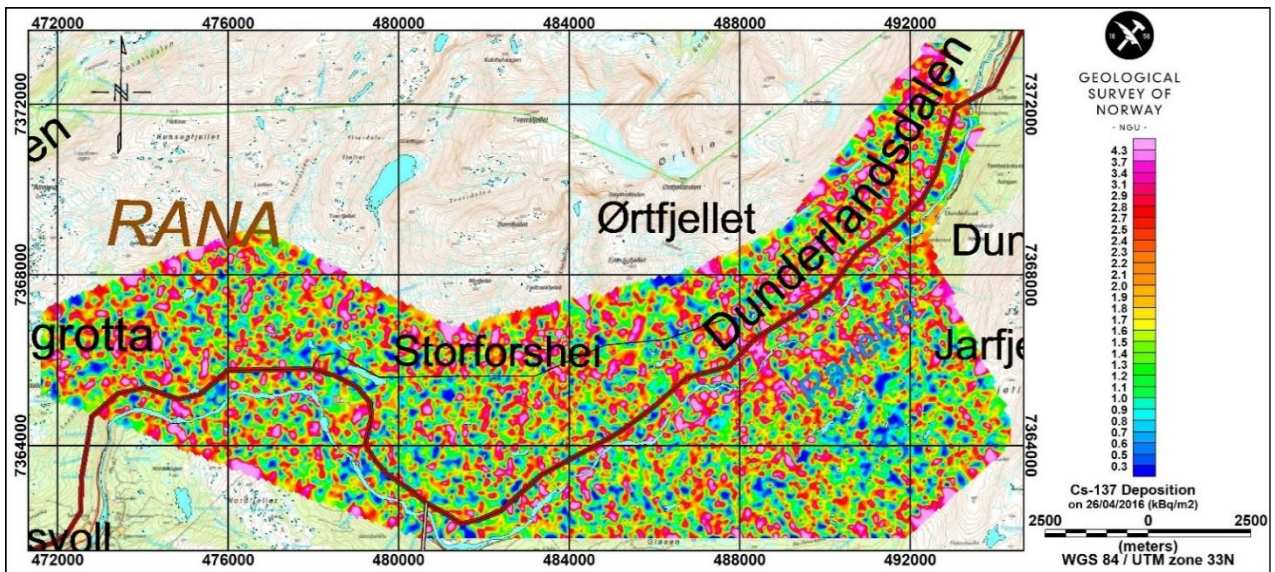

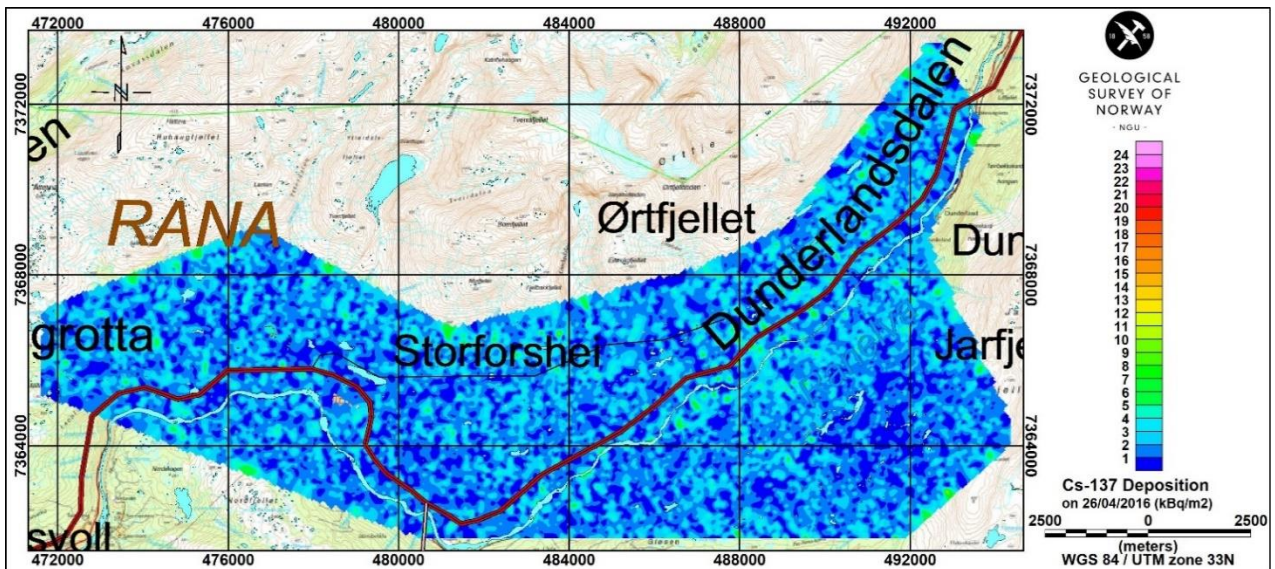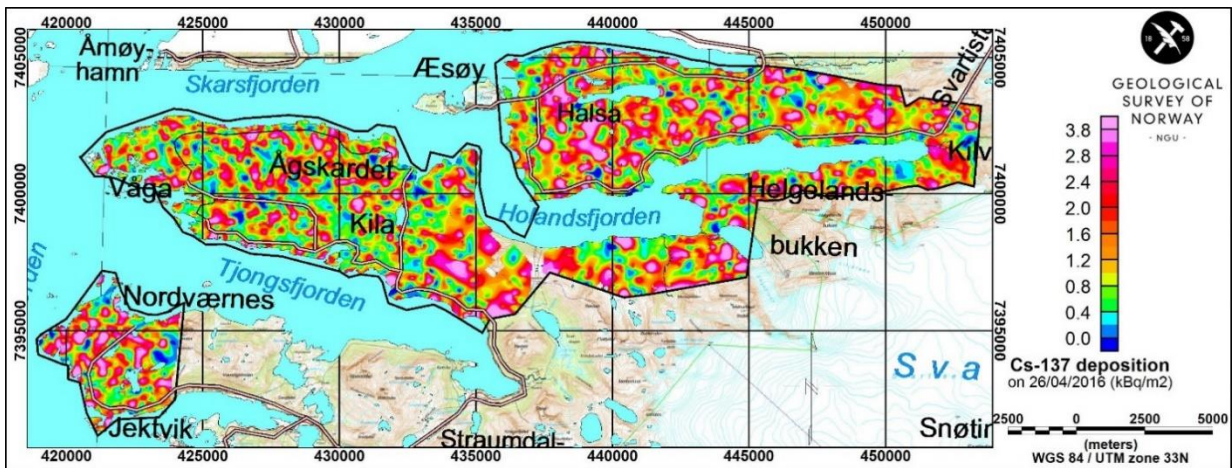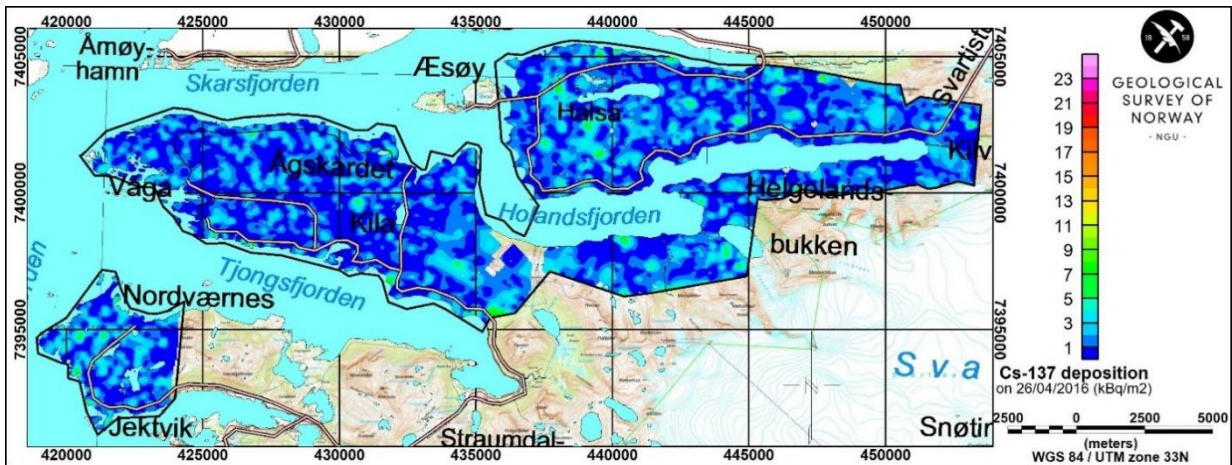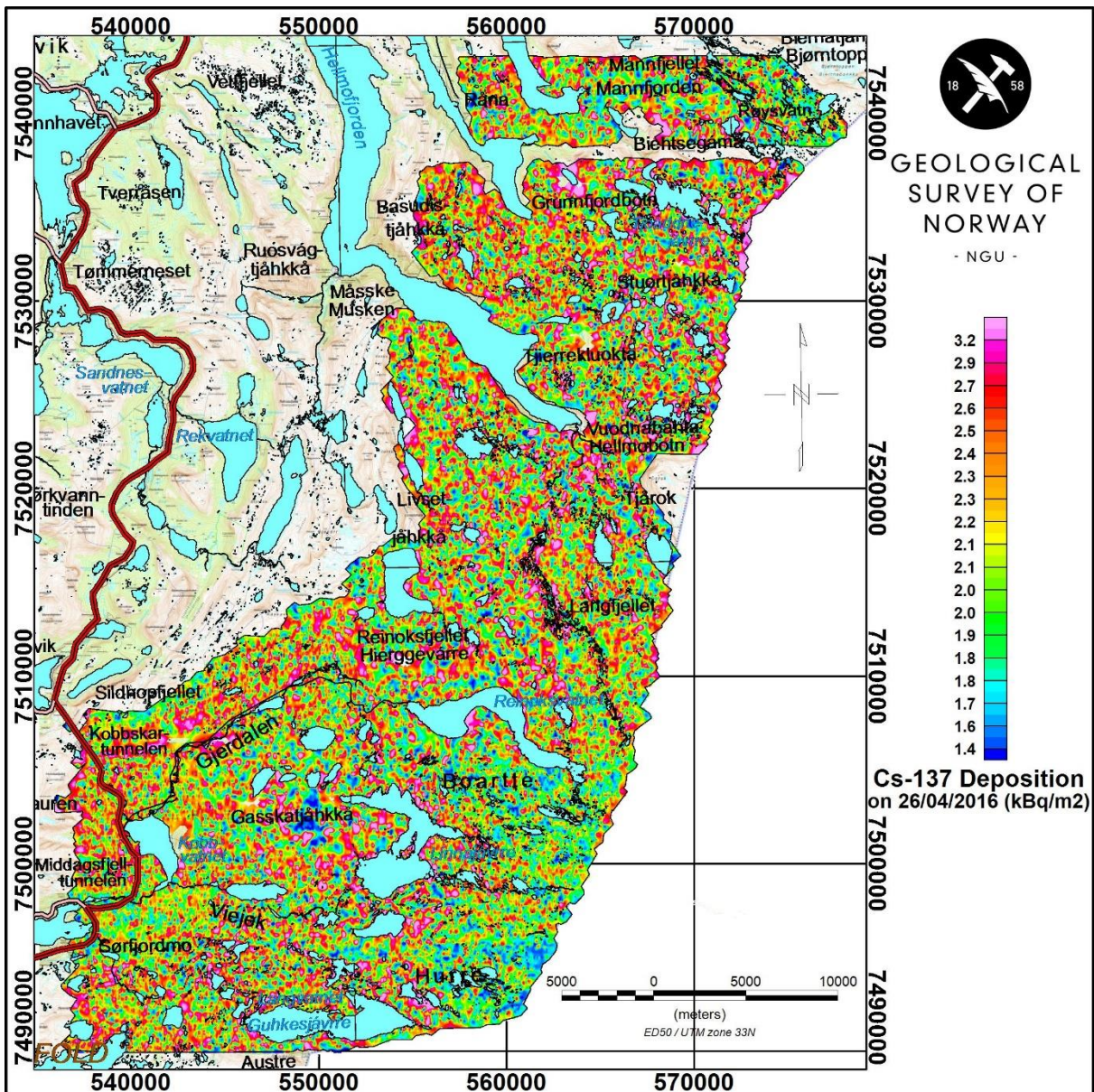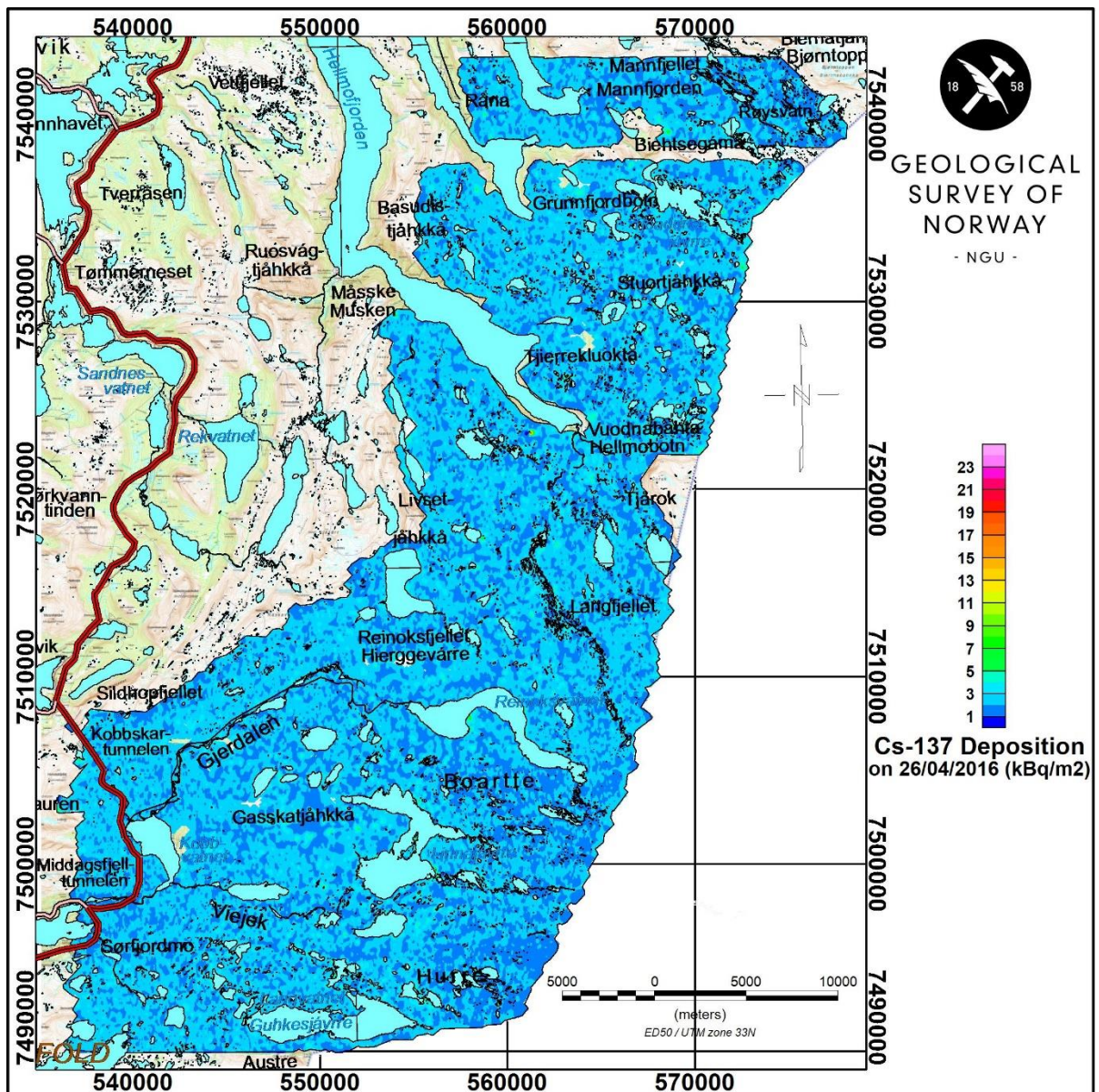Figure 36: Cs-137 ground deposition in histogram equalisation scale from the Hellemobotn area.

Figure 37: Cs-137 ground deposition in linear scale from the Hellemobotn area.

5. DISCUSSION

We developed a more reliable processing for Cs-137 concentration calculation from airborne gamma-ray spectrometry data using a new calibration to calculate sensitivity coefficient and following the approach of Oberlercher and Seiberl (1997). Following the recalibration and reprocessing, we produced and presented several Cs-137 maps from various parts of Norway. There were several problems with the methodology of Cs-137 concentration calculations applied to the Jotunheimen data in 2011.

1. In earlier processing of the Jotunheimen data, we used a height attenuation coefficient derived from an area where concentration of Cs-137 was very low which led to an unreliable height attenuation factor for Cs-137.
2. The height attenuation coefficient was calculated from the data collected for altitudes between 40 m and 150 m, but it was used to correct Cs window counts at 60 m (and above) to the ground concentrations. The height-dependent relationship derived from 40 m -150 m data may not be applicable for 60 m to the ground.
3. Calibration to calculate sensitivity coefficient was performed using a Cs-137 point source (433 kBq) placed at various locations in a grid pattern (within a few meters of the detector) to approximate a uniform surface distribution, and did not adequately considered the full spatial (3D) distribution of a surface deposition.
4. The 2011 calibration did not account for the penetration of Cs-137 into the soil that had occurred during the 25 years after the fallout, resulting in increased shielding by the soil (ICRU 1994).

Due to all these reasons, when we compared *in situ* Cs-137 deposition and measured by helicopter, then we observed that Cs-137 deposition by helicopter-borne measurements was underestimated by a factor of ca. 1.6. Therefore, we planned for a recalibration survey from a high Cs-137 area in Beitostølen. Following all the steps properly as described in Chapter 3.2, we obtained a one to one correlation between Cs-137 deposition by *in situ* and helicopter-borne measurements. Though small and local variabilities were still present in the field as it discussed in detail by Thørring et al. (2019).

Reprocessing of older spectrometry data was complicated by factors including missing or poor-quality GPS and altitude data, and excessive noise in the data. The data were manually inspected and corrected. All the calibration parameters were not available for all the old surveys, so calibration parameters from the years and areas nearby were used. A few lines from Frosta in 2015 were flown to make sure that we have some overlapping areas between old helicopter-borne surveys, TRAS-12 fixed- wing survey and new helicopter-borne surveys. Cs-137 concentrations from these overlapping areas were used to perform regression analyses to find the coefficients for various areas so that they could be levelled to match with the correct estimation of Cs-137 obtained from the recent surveys.

In some of old data from Nordland and Trøndelag, we always see a peak around 609 keV (specially in Hellemobotn) in the spectra which is a peak for low energy Bi-214 from daughter product of natural uranium (i.e. U-238). This peak could be easily mistaken as Cs-137 peak (at 662 keV) when Cs concentrations are low, and spectrum is not very clean for every observation point. However, it is very clear from Røyrvik and Skorovatn (in Trøndelag) that when Cs-137 is present then it has a clear peak at 662

keV and not at ca. 609 keV even if the spectrum is not very clean at each observation point. A running average or general average of the spectra for few observation points e.g. 30 shows the radio-peaks more clearly.

In the processing of fixed-wing TRAS-12 data, radar altimeter data for higher altitude as more than 240 m is set to 240 m. If Cs-137 radiation was observed at higher flying altitude (more than 240 m) for TRAS-12 survey, then it would result in much higher ground deposition than we would obtain by assuming its collection at 240 m altitude. Another problem with TRAS-12 data was that they performed height attenuation calibration for Cs-137 between 0 to 160 m (Novatem 2014b), however this height attenuation coefficient was used to attenuate/elevate the Cs-window counts from 30 to 240 m heights to 120 m nominal height which might result in wrong level of Cs-137 ground deposition. These could be the reason that the TRAS-12 data showed rather low ground deposition of Cs-137 in Trøndelag and it was needed to be multiplied with 4.7 to match it to the level of Cs-137 deposition calculated from Frosta using helicopter-borne data in 2015 (details in Chapter 4.3.2).

Raw counts collected by AGRS are positive (or zero) but they contain some inherent statistical noise due to the nature of the radioactive decay. As we process the data, and apply corrections, the noise envelope widens and leads to negative values. Therefore, we replace negative values to dummy at several stages of the processing.

We adopted the procedure of Compton continuum removal from Cs-137 window from Oberlercher and Seiberl (1997) but still we could not completely remove all the contributions from the decay chain of U from Cs-137 window. When we closely observed spectra from Høgtuva and other places where we calculated final Cs-137 concentration to be < 5 kBq/m^2, we could not observe any Cs-137 peak in the spectra. However, we clearly observed a peak at ca. 609 keV which could be either from Bi-214 or Cs-134. Cs-134 has half-life of two years only so it should have been decayed to a not detectable minimum after eleven years since the accident. The concentration of ca. 5 kBq/m^2 or less observed for Cs-137 is either from Cs-134 or from Bi-214 (daughter product of U). Therefore, we assume that 5 kBq/m^2 or lower concentration of Cs-137 is below the noise level. This means that Cs-137 concentrations at Hellemobotn, Høgtuva, Rana and Holandsfjord are below the noise level. The Cs-137 concentrations in the areas Røssvatnet, Korgen, Hjartfjellet and Oppdal indicate some Cs-137 in these areas but not as high as in Jotunheimen, Hattfjelldal and Trøndelag. The areas Jotunheimen-Otta-Vågå, Trøndelag and Hattfjelldal have still a high Cs-137 deposition concentration and it is well above the noise limit.

6. CONCLUSION

Cs-137 deposition maps are produced using airborne spectrometry data from Nordland, Jotunheimen and Trøndelag which are considered to be mostly affected after the Chernobyl nuclear accident in 1986. Airborne data were collected in different surveys using helicopter-borne and fixed-wing aircrafts during 1987 to 2015. Recalibration and reprocessing methods are demonstrated to correct low energy isotopes from U and Th decay chain appearing in Cs-137 window and to find a better correlation between airborne and *in situ* measurements. Two examples from low and high Cs-137 deposition areas effectively demonstrate the effectiveness of reprocessing method in removing trend of natural radioelements from Cs-137 concentration, especially in low Cs-137 area. Recalibration data from Beitostølen, Jotunheimen brought estimation of Cs-137 from airborne measurements to almost equal to *in situ* measurements regardless of local variations and different scale of these two measurements.

Airborne radiometry data are reprocessed according to the new calibration and reprocessing procedures using sensitivity coefficient calculated from the Beitostølen calibration data. The sensitivity coefficient can be different in other areas depending on soil density and depth distribution profile of Cs-137 from that area. In Hattfjelldal and Jotunheimen there are many areas that are still contaminated with presence of high amount of Cs-137 (up to 150 kBq/m^2 obtained from airborne measurements) even 30 years after the nuclear accident. The Cs-137 concentration is ca. 10 kB/m^2 at some places in Røssvatnet-Korgen-Hjartfjellet and Oppdal areas. Other areas in Nordland county (Høgtuva, Rana, Holandsfjord and Hellemobotn) show lower Cs-137 contamination below noise level. The Trøndelag area, as it is measured from airborne surveys, shows contamination of 20 to 50 kBq/m^2 in some of the areas whereas other areas are not contaminated.

Cs-137 deposition is calculated for the actual survey year and then concentration is calculated for year 2016 using the half-life decay equation. There could be additional washing of the deposited Cs-137 or other changes due to agriculture or other activities in some of the areas. Therefore, the original Cs-137 could be different than the decay-corrected concentration of 2016 Cs-137 level.

7. REFERENCES

Baranwal, V.C. 2016: Compilation of various airborne geophysical data in the Oslofjord area. NGU report no. 2013.030, pp. 38.

Baranwal, V.C., Ofstad, F., Rønning, J.S. & Watson, R.J. 2011: Mapping of caesium fallout from the Chernobyl accident in the Jotunheimen area. NGU report 2011.062, pp. 26.

Beard, L.P. & Mogaard, J.O., 1999: Data acquisition and processing - Helicopter geophysical survey, Røros. NGU report no. 99.118, pp. 14.

De Cort, M., Dubois, G., Fridman, S.D., Germenchuk, M.G., Izrael, Y.A., Janssens, A., Jones, A.R., Kelly, G.N., Kvasnikova, E.V., Matveenko, I.I., Nazarov, I.M., Pokumeiko, Y.M., Sitak, V.A., Stukin, E.D., Tabachny, I.Y., Tsaturov, Y.S. & Avdyushin, S.I. 1998: Atlas of Caesium Deposition on Europe after the Chernobyl Accident. EUR 16733. European Commission, Luxembourg, pp. 176.

Dumais, M.-A. 2014: Reprocessing and compilation of radiometric data from Finnmark and northern Troms. NGU report no. 2014.015, pp. 48.

Geosoft, 2018: Oasis Montaj 9.4: Mapping and Processing System. Geosoft, Toronto, Canada.

Grasty, R.L. & Minty, B.R.S. 1995: A guide to the technical specifications for airborne gamma-ray surveys. Australian Geological Survey Organisation (AGSO), Record 1995/60.

IAEA 1991: Airborne Gamma Ray Spectrometer Surveying. IAEA Technical Reports Series No. 323, pp. 97.

IAEA 2003: Guidelines for radioelement mapping using gamma ray spectrometry data. IAEA-TECDOC-1363, Vienna, Austria, pp. 173 pp.

ICRU 1994: Gamma-ray spectrometry in the environment (report 53). International Commission on Radiation Units and Measurements, Bethesda, Maryland.

Isaksson, M. 2011: Environmental Dosimetry – Measurements and Calculations, Radioisotopes - Applications in Physical Sciences, Prof. Nirmal Singh (Ed.), IntechOpen.

Lindahl, I. & Håbrekke, H. 1986: Kartlegging av radioaktivt nedfall etter Tsjernobylulykken 1986. NGU Rapport 86.160 (in Norwegian).

Mauring, A. 2016: Feltarbeid i Jotunheimen med NGU sommeren 2015, unpublished technical report, DSA, pp. 21.

Mauring, A., Vidmar, T., Gafvert, T., Drefvelin, J. & Fazio, A. 2017: InSiCal – a tool for calculating calibration factors and activity concentrations in in situ gamma spectrometry. J. Environ. Radioact., 188, p.58-66.

Mogaard, J.O. & Blokkum, O. 1993: Geofysiske målinger fra helikopter over Meråkerfeltet, Nord-Trøndelag NGU report no. 92.153, pp. 9 (in Norwegian).

Mogaard, J.O., 1992: Geofysiske målinger fra helikopter over et område i indre Tysfjord, Nordland, NGU report no. 92.229, pp. 9, (in Norwegian).

Mogaard, J.O., 1993: Helicopter Survey over Gråurdfjellet, Sør-Trøndelag, Norway. NGU report no. 93.137, pp. 13, (in Norwegian).

Mogaard, J.O. & Olesen, O., 1997: Geofysiske målinger fra helikopter ved Bleikvassli, Nordland, NGU report no. 96.050, pp. 35, (in Norwegian).

Mogaard, J.O., Rønning, S., Blokkum, O. & Kihle, O. 1989: Helikoptermålinger kartblad Steinkjer, Nord-Trøndelag, NGU-rapport no. 89.142, pp 30, (in Norwegian).

Mogaard, J.O., Rønning, S. & Blokkum, O. 1988: Geofysiske målinger fra helikopter over et område rundt Høgtuva, Nordland, NGU report no. 88.157, pp. 25, (in Norwegian).

Novatem, 2014a: Operations report: Fixed-wing magnetic and radiometric survey over the Trøndelag coastal area in Central Norway, Trøndelag region airborne survey (TRAS -12), Report no. C12095/NGU–TRAS-12, Norway 2012 & 2013, pp. 29.

Novatem 2014b: Calibration report: Airborne magnetic and radiometric survey, Norges Geologiske Undersøkelse (NGU), Trøndelag region airborne survey: TRAS-12 Norway 2011-2014, report no. C12095_ngu, pp. 46.

Oberlercher, G. & Seiberl, W. 1997: Quantitative Cs-137 distribution from airborne gamma ray data, IAEA report, IAEA-TECDOC-980.

Ofstad, F. 2015. Helicopter-borne magnetic and radiometric geophysical survey in Otta and Vågå area, Sel and Vågå municipalities, Oppland County. NGU Report no. 2015.058, pp. 27.

Rodionov, A., Ofstad, F. & Tassis, G. 2012: Helicopter-borne magnetic, electromagnetic and radiometric geophysical survey in the Storforshei area, Rana, Nordland, NGU report no. 2012.044, pp. 31.

Rodionov, A., Ofstad, F. & Tassis, G. 2013: Helicopter-borne magnetic, electromagnetic and radiometric geophysical survey in Holandsfjorden area, Meløy, Nordland, NGU report no. 2013.043, pp. 26.

Rodionov, A., Ofstad, F., Stampolidis, A. & Tassis, G. 2014: Helicopter-borne magnetic, electromagnetic and radiometric geophysical survey in Hattfjelldal, Nordland County. NGU Report 2014.029, pp. 29.

Rodionov, A., Ofstad, F., Stampolidis, A. & Tassis, G. 2016: Helicopter-borne magnetic, electromagnetic and radiometric geophysical survey in Gauldal and Sokndal area, Sør Trøndelag County. NGU report no. 2015.053, pp. 31.

Rønning, J.S., Walker, P., Kihle, O. & Mogaard, J.O. 2002: SKB site investigations. Helicopter borne geophysics at Simpevarp, Oskarshmn, Sweden, NGU report no. 2002.094, pp. 58.

Rønning, S. 1991: Helikoptermålinger over kartblad Andorsjøen 1823 I, NGU report no. 91.153, pp. 14, (in Norwegian).

Rønning, S. 1992a: Helikoptermålinger over kartblad 1823 III, Snåsa. NGU report no. 92.144, pp. 13, (in Norwegian).

Rønning, S. 1992b: Helikoptermålinger over kartblad 1723 II, Snåsavatnet. NGU report no. 92.145, pp. 13, (in Norwegian).

Rønning, S. 1992c: Helikoptermålinger over kartblad 1723 I, Overhalla. NGU report no. 92.146, pp. 13, (in Norwegian).

Rønning, S., 1995a: Helikoptermålinger over kartblad 1722 IV, Stiklestad, NGU report no. 93.084, pp. 13, (in Norwegian).

Rønning, S. 1995b: Helikoptermålinger over Fosenhalvøya, kartbladene 1622 I-IV og 1623 II og I, NGU report no. 95.064, pp. 19, (in Norwegian).

Rønning, S. 1995c: Helikoptermålinger over Grongfeltet, Nord-Trøndelag 1993 og 94. NGU Report no. 95.057, pp. 14 (in Norwegian).

Rønning, S., Kihle, O., Blokkum, O. & Håbrekke, H. 1990: Helikoptermålinger kartblad GRONG og sydlige halvpart av kartblad HARRAN, NGU report no. 90.085, pp 22 (in Norwegian).

Skilbrei, J.R. 1994: Helikoptermålinger i Vuku-området, Steinkjer og Verdal kommuner, Nord-Trøndelag, NGU report no. 93.104, pp. 18, (in Norwegian).

Stampolidis, A. & Ofstad, F. 2015. Helicopter-borne magnetic and radiometric geophysical at Drangedal, Telemark County. NGU Report 2014.044 (29 pp.).

Stampolidis, A. & Ofstad, F. 2016: Helicopter-borne magnetic, electromagnetic and radiometric geophysical survey in Steinkjer, Nord-Trøndelag. NGU report no. 2015.060, pp. 31.

Thørring, H., Baranwal, V.C., Ytre-Eide, M.A., Rønning, J.S., Mauring, A., Stampolidis, A., Drefvelin, J., Watson, R.J. & Skuterud, L. 2019: Airborne radiometric survey of a Chernobyl-contaminated mountain area in Norway - using ground-level measurements for validation. J. Environ. Radioact., 208-209, p. 1-11.

Thørring, H.& Skuterud, L. 2012: Ground deposition of Cs in Jotunheimen and Valdres. Presentation at a meeting at NGU 26.11.2012.

Tyler, A.N., Sanderson, D.C.W., Scott, E.M. & Allyson, J.D. 1996: Accounting for Spatial Variability and Fields of View in Environmental Gamma Ray Spectrometry, J. Environ. Radioact., 33, No.3, pp 213-235.

Walker, P. 1992: A geophysical investigation of Kjølhauggruppen and Sulåmogruppen over two areas near Meråker, Norway, NGU report no. 92.270, pp. 14.

Walker, P. & Smethurst, M.A. 1993: The distribution of ^{137}Cs in the Meråker and Grong/Snåsavatnet Areas, Nord-Trøndelag, NGU report no. 93.045, p44.

Wilford, J. 2002: Airborne gamma-ray spectrometry. Geophysical and Remote Sensing Methods for Regolith Exploration, CRCLEME Open File Report. 144.

GEOLOGICAL
SURVEY OF
NORWAY

· NGU ·